AFCRL-67-0633

EXTENDED DYNAMIC RANGE PROCESSING

By

A. Shepp, W. Kammerer, and R. Shuman

Technical Operations, Inc.
South Avenue, Burlington, Mass. 01803

Contract No.: F1962867C0082

Project No. 8663

Task No. 866300

Unit No. 86630001

FINAL REPORT

Period Covered: 10 October 1966 through 10 October 1967

November, 1967

Contract Monitor: George A. Vanasse
Optical Physics Laboratory

Prepared
for

AIR FORCE CAMBRIDGE RESEARCH LABORATORIES
OFFICE OF AEROSPACE RESEARCH
UNITED STATES AIR FORCE
BEDFORD, MASSACHUSETTS 01730

This research was supported by the Advanced Research Projects Agency under ARPA Order No. 450

AFCRL-67-0633

EXTENDED DYNAMIC RANGE PROCESSING

By

A. Shepp, W. Kammerer, and R. Shuman

Technical Operations, Inc.
South Avenue, Burlington, Mass. 01803

Contract No.: F1962867C0082

Project No. 8663

Task No. 866300

Unit No. 86630001

FINAL REPORT

Period Covered: 10 October 1966 through 10 October 1967

November, 1967

Contract Monitor: George A. Vanasse
Optical Physics Laboratory

Prepared
for

AIR FORCE CAMBRIDGE RESEARCH LABORATORIES
OFFICE OF AEROSPACE RESEARCH
UNITED STATES AIR FORCE
BEDFORD, MASSACHUSETTS 01730

This research was supported by the Advanced Research Projects Agency under ARPA Order No. 450

ABSTRACT

Four Kodak films — Pan-X, Plus-X, Tri-X, and High-Speed Infrared — were exposed to slit images (1.7 x 14 mm) over a range of 10^4 E. Samples were developed in D-19 and D-76 for high- and low-contrast control and in three Tech/Ops extended dynamic range (XDR) developers — E-20A, E-20B, and Type IV. Subsequent analyses showed that the XDR developers produce lower granularity than the control developers and thus greatly reduce the apparent flare and increase detectivity, even at low density and gamma.

TABLE OF CONTENTS

BLANK PAGE

LIST OF ILLUSTRATIONS

LIST OF ILLUSTRATIONS (Cont'd.)

LIST OF CONTRIBUTING SCIENTISTS

A. Shepp
W. Kammerer
R. Shuman
B. Justh
R. Langer

LIST OF RELATED CONTRACTS AND PUBLICATIONS

1. RADC, Contract No. AF 30(602)-3227.
A. Shepp, L.D. Corben, and D.L. Davidson, "Film Investigation (U)," Technical Operations, Inc., Report No. TO-B 64-101 (RADC-TR-64-522) May 1965 (Secret).

2. RADC, Contract AF 30(602)-4279
W. Kammerer, L.Corben, and others, "Extended Dynamic Range Process," Technical Operations, Inc., Report No. TO-B 67-37 (RADC-TR-67-431) (1967).

SECTION I

INTRODUCTION AND SUMMARY

On this program, we have studied the photographic development of overexposed images, using developers that apparently reduce flare, leading to more accurate measurement of image dimensions, and allowing more accurate photometric interpretation of the images.

These "Extended Dynamic Range" (XDR) developers were first formulated in our laboratories, in part under earlier government programs[1, 2] supported by Rome Air Development Center and in part by independent research at Tech/Ops. These XDR developers, as a class, develop conventional films to low densities and gammas without an undue loss of toe speed (low light-level sensitivity). They also have the unusual property of allowing the developed film to show a continual rise in density with increasing exposure, over an extended exposure range of up to 10^6 E, without exceeding a D_{max} of 2.0. Similarly, if the conventional films studied (Kodak films Pan-X, Plus-X, Tri-X, and High Speed Infrared) are given a strong image overexposure (that is, are used to record a wide dynamic range within one exposure) then the XDR developers, in contrast to the control developer, bring up the image with an apparent reduction of flare and increase in detectivity. As a result of the work performed on the present program, we attribute the reduction of flare largely to a reduction of the granularity of the image produced by the XDR developer.

This program has been supported by the Advanced Research Projects Agency (ARPA) through the Air Force Cambridge Research Laboratory (AFCRL). It has been performed in conjunction with a related program, supported by Rome Air Development Center (RADC), now concluded.[2] This dual support resulted from the diversified interests of the two agencies. The program supported by RADC was devoted to extended exposure-latitude studies. In the final report of that program,[2] we presented extended exposure-latitude results for XDR developers on specific films, as a function of resolution, and in terms of new extended range functions. The present program, supported by ARPA-AFCRL, concerns the application of XDR developers to specific films for the recording of wide dynamic range exposures and the reduction of flare. The RADC report[2] should be read in conjunction with this present one for a more complete understanding of XDR developer performance, and for convenience, some of the sensitometric and resolution data of that report are included here.

The results of this present program would appear to be applicable to the photographic recording of strongly illuminated or self-luminous objects whose dimensions and surface temperatures are to be determined by photographic measures. Photographic tests of this type have been performed on this program in cooperation with the Lincoln Laboratory, but the results of these tests are not available for inclusion in this report.

The major findings of this program may be summarized as follows:

1. Four conventional films (Kodak Pan-X, Plus-X, Tri-X, and High Speed Infrared) were exposed to slit images (1.7 x 14 mm), whose exposure range varied over 10^4 E. Qualitatively, the flare appears to be greatly reduced by the use of XDR

developers. This was checked by low power (8 X) observations of the slit images, and by high power (20 X) microdensitometer measurement of the images. At low power, the measured values for the XDR-developed slit widths remained accurate to 12% (1.7 to 1.9 mm on the film), as a function of the 10^4 exposure range, while the measured values on the control-developed (D-19) exposures quickly became inaccurate and finally unmeasurable at heavy exposures.

The microdensitometer traces of the developed slit images did not allow for an accurate determination of the slit width because of complex edge effects.

2. Microdensitometer traces of the developed slit images showed that XDR processing produced a lower granularity than the control, and this makes a major contribution to the decreased flare and increased detectivity associated with XDR processing.

(a) The flat density portions of the scanned slit images show fewer fluctuations than the control at constant scanning aperture (i.e., lower granularity). This gives the image an appearance of reduced flare and should enable one to make more accurate photometric readings of the images.

(b) The fewer fluctuations of the scanned image (lower granularity) are interpretable in terms of increased detectivity. In the numerous photographs of high intensity objects taken in our laboratory (such as that of the projection lamp shown in Figure 14 below) more image discrimination is observed on the XDR-developed images than on the control-developed images.

3. The XDR-developed slit images show a sharp edge enhancement easily seen on the microdensitometer traces that does not appear on the control traces. This effect seems to contribute to the greater accuracy with which we can measure the dimensions of the XDR-processed slit widths at low power.

4. The XDR development in wide exposure-range studies of sensitometry and resolution produces peak resolution values that are comparable or superior to those of the control development. More important, it gives high resolution over a greater exposure or intensity range than do the control developers. We attribute this in large part to the reduced granularity of the XDR developers, which can make up for the apparent loss of contrast (lowering of gamma) produced by these developers.

5. The XDR processing of the films studied on this program gives reduced density, gamma, and toe speed compared with control processing. But the lower granularity of XDR development allows the films to show high detectability even at low density and gamma. The lower toe speed is of consequence only in the region of very low level exposures. We have not done extensive testing of detectability in this region.

In the sections that follow, we shall first present a summary of sensitometric and resolution data taken at low intensity exposure, that sums up the wide latitude and range capability of the developers. We shall next introduce the quantitative concepts of granularity and detectivity as an introduction to our flare studies. Finally, we shall present our experimental flare work, and draw conclusions based on the relationship between XDR development characteristics and granularity theory.

SECTION II

SENSITOMETRIC AND RESOLUTION RESULTS

EXPERIMENTAL

At the outset of this report, we shall first summarize the sensitometric and resolution data obtained on films of interest, for control and XDR developers, under conditions of low intensity and extended exposure time. These results will be summarized in Tables I and II and in Figures 1-10.

Film Types

In Table I, we list the four Kodak films studied on this program. These films were chosen because they are the film types most used by the Lincoln Laboratory in the field photography of highly illuminated objects. The Lincoln Laboratory task involves the recording of spectra, the photometric reduction of data, and some measurement of object dimensions.

TABLE I

DEVELOPER FORMULATIONS USED IN THIS REPORT

(g/liter)

Formulation	T/O XDR Developers			Kodak Developers	
	E-20A	E-20B	Type IV	D-19	D-76
K_2SO_3	25	50	25	–	–
Na_2SO_3	–	–	–	90.0	100.0
Metol (Elon)	0.5	0.5	0.5	2.0	2.0
Hydroquinone (HQ)	0.5	0.5	0.5	8.0	5.0
K_2CO_3	–	–	10.0	–	–
Na_2CO_3	–	–	–	52.5	–
Borax	–	–	–	–	2.0
KBr	–	–	–	5.0	–
Kodak Film Type	Recommended T/O Developer				
Pan-X	X		X		
Plus-X			X		
Tri-X			X		
High Speed IR		X			

Developer Formulations

In Table I, we also show the formulations of three XDR developers: T/O E-20A, E-20B, and Type IV, as well as those for the two control developers: Kodak D-19 (Air Force high contrast) and D-76 (Air Force low contrast).

All the developers of Table I are superadditive in Hydroquinone (HQ) and Metol, stabilized with sulfite ion. In this common type of developer, Metol (p-methylaminophenol) initiates development and, upon being oxidized, is regenerated by HQ. Oxidized HQ is stabilized by sulfite ion to form the nonstaining sulfonate. These developers show constant activity (due to regeneration) and remain clean throughout development. The high activity of D-19 and D-76 is established by the high ratio of HQ to Metol, and by the relatively high alkalinity set by carbonate in D-19 and by borate in D-76. The high activity of D-19 requires the presence of bromide ion as a development restrainer.

In the XDR developers, activity is greatly reduced by the use of a low HQ-to-Metol ratio and by very moderate pH (set by sulfite alone in E-20A and E-20B and by a low carbonate concentration in Type IV). However, the use of HQ-Metol does give sufficient developer activity to establish a good toe speed and to allow for the development of good density at high exposure.

Exposure Step Tablets

The XDR developers produce extremely low tonal densities over a 10^3 E exposure range. To properly present the characteristics of these developers, a step tablet that covered 10^6 E units was made from a normal 21 step No. 2 tablet (35 mm x 6 in.) by placing a No. 3 neutral density filter along one half the length of the tablet. In this manner, the new tablet showed 41 steps of different density from 0 to 6.0 (step 21 = step 22) covering an attenuation of 10^6 (6 log E). On each of the 41 steps, a USAF 1951 High Contrast 3-bar resolution (bar density = 2.0) was superimposed by a careful printing procedure. Therefore, by photographing an experimental film in contact with this 41-step resolution wedge, both a characteristic curve and a high-contrast resolution curve could be exposed. The resolution values determined by this method cannot claim to be the maximum resolution of which the film is capable, primarily because of contact exposure problems. However, the resolution-log E curves we have obtained show the exposure range of resolution, and the values are accurate on a relative basis.

Sensitometric Exposures

Each film tested was exposed to the XDR resolution step tablet in a Tech/Ops calibrated white-light sensitometer.[3] The lamp was corrected to 5500°K with a standard blue filter. The unattenuated light intensity on the film plane was 125 mc (metercandles). To ensure that the test films received enough exposure, the exposure time was set at 10 sec, so that the unattenuated exposure striking the film was 1250 mcsec. Since the step tablet had an attenuation of 10^6 E, the exposure on the first step (most attenuated) was 0.00125 mcsec, so that Abs log E = 7.10-10.

The maximum intensity of 125 mc on the film plane of the sensitometer is only reasonably high. Therefore, in the slit experiments to be described below, the (mercury lamp) intensity was set about 10-fold higher, I = 1250 mc, so that an exposure of the slit image of 1 sec produced an exposure of 1250 mcsec on the film, which is quite intense, and caused severe overexposure on all films tested.

Processing and Reading

Exposed wedges were developed in D-19 undiluted for 4 min at 68°F for a high-contrast control and in D-76 (diluted 1:1) for 4 min at 68°F for low-contrast control. The three T/O XDR developers were all used at 4 min, 68°F. In all cases, tray processing with hand agitation was used.

Densities were read in the diffuse manner on a MacBeth Quantascan densitometer. Resolution was read by microscope observation of the developed targets—the highest resolved target on each step was recorded.

Characteristic Curve–Resolution Paper

A new XDR sensitometric-resolution chart paper was designed for use in this work[2] (see Figures 1-8). The lower horizontal coordinate is log E, covering a range of 0 to 6. The upper horizontal coordinate consists of 41 steps superposed on the log E scale. The left-hand vertical coordinate is density and is linear with log E. The right-hand vertical coordinate is resolution in lines/mm, read as the maximum resolution target on each step, observed by microscopic examination.

This chart paper is used in the D-log E mode in Figures 1, 3, 5, and 7 and is used in the resolution-log E mode in Figures 2, 4, 6, and 8. This presentation of resolution data is especially interesting and is standard in our laboratories, since it shows the exposure range over which a resolution value is maintained by the developed film.

RESULTS

Characteristic and Resolution Curves

Figure 1 shows a set of characteristic curves for Pan-X, and Figure 2 shows the resolution-log E curves for the same film. The behavior of these curves is characteristic of the other three films studied, as shown in Figures 3 to 8. In Figure 1, the D-19 curve would appear to show as great a latitude as the other curves, but much of this latitude is at densities above 2.0. Observe in Figure 2 that the D-19 resolution curve peaks below the others, and starts to fall at log E values of 3.3 and above, at which the density (Figure 1) is 2.6 and above. The D-76 curve would appear to have a latitude equal to that of E-20A and Type IV, but this latitude is obtained at higher density. The detective superiority of E-20A and Type IV over D-76 is shown in Figure 2, where we find that the peak resolution values for all three developers is about the same, but the log E range of higher resolution values is much broader for the XDR developers than for D-76.

In Figures 3 and 4, data for Plus-X are plotted. The D-19 curve for this developer quickly goes to high density, and the resolution curve is accordingly quite low. Again, the range of D-76 appears to be comparable to that of Type IV. On this film, E-20A seems to be too slow for effective use. However, the resolution data of Figure 4 show E-20A to be the superior high-resolution developer, with Type IV having an equally wide range at 70 ℓ/mm.

The behavior of Tri-X, shown in Figures 5 and 6, is similar to that of Plus-X.

EXTENDED RANGE PAPER

DATE 67

PREPARED

FILM Pan-X

MANUFACTURER EK

SENSITOMETER

EXPOSURE TIME 10

DEVELOPER

DEV. TIME 4m AT 70 °F

DEVELOPMENT CONDITIONS

SENSITOMETRIC PROPERTIES

BASE DENSITY

SPEED AT D

GAMMA

ABS LOG E 7.10-10

tech ops

TECHNICAL OPERATIONS, INCORPORATED
BURLINGTON, MASSACHUSETTS

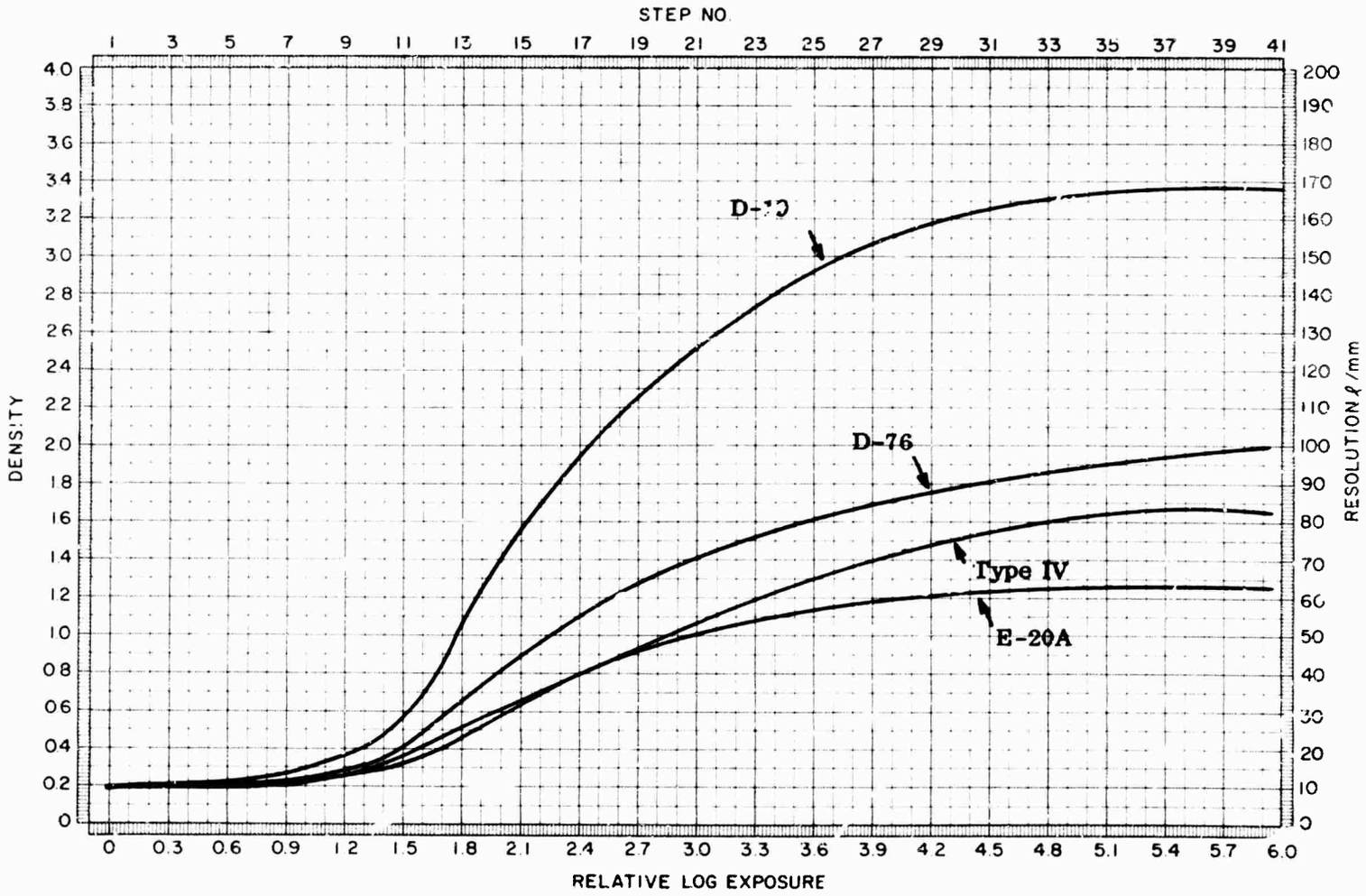

Figure 1. Characteristic Curves for Pan-X, Developed in D-19, D-76 (1:1), XDR Type IV, and XDR E-20A

EXTENDED RANGE PAPER

DATE 67

PREPARED BY

FILM Pan-X

MANUFACTURER EK

SENSED X

EXPOSURE TIME 10 SEC.

DEVELOPER

DEVELOPMENT 4m AT 70 °F

DEVELOPMENT CONDITIONS

8

SENSITOMETRIC PROPERTIES

BASE DENSITY

SPEED AT D

GAMMA

ABS LOG E

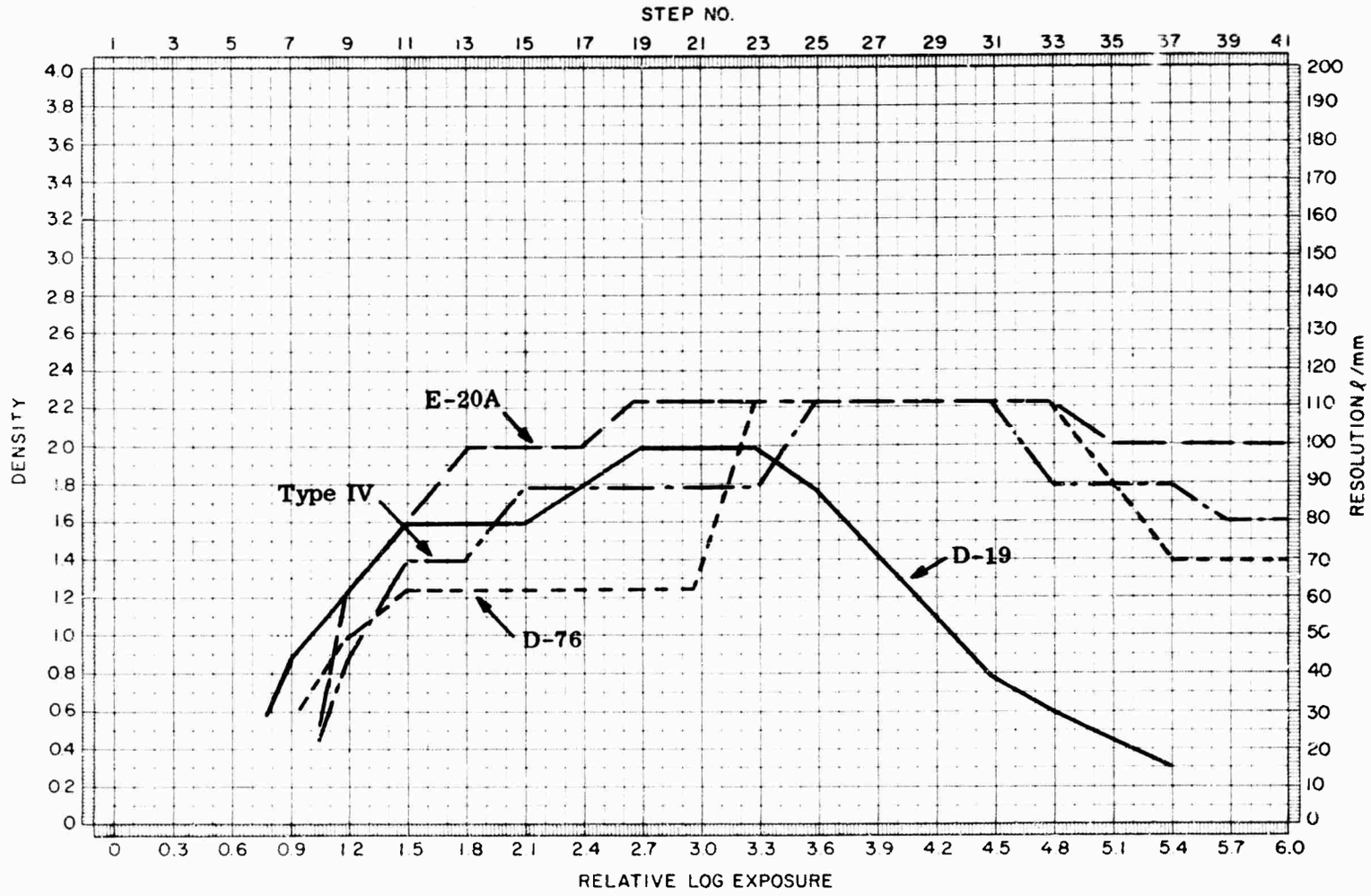

Figure 2. Resolution Curves for Pan-X, Developed in D-19, D-76 (1:1), XDR Type IV, and XDR E-20A

TECHNICAL OPERATIONS, INCORPORATED
BURLINGTON, MASSACHUSETTS

67

Plus-X
EK

10

4m 70

6

7.10-10

tech ops

TECHNICAL OPERATIONS,
INCORPORATED
BURLINGTON, MASSACHUSETTS

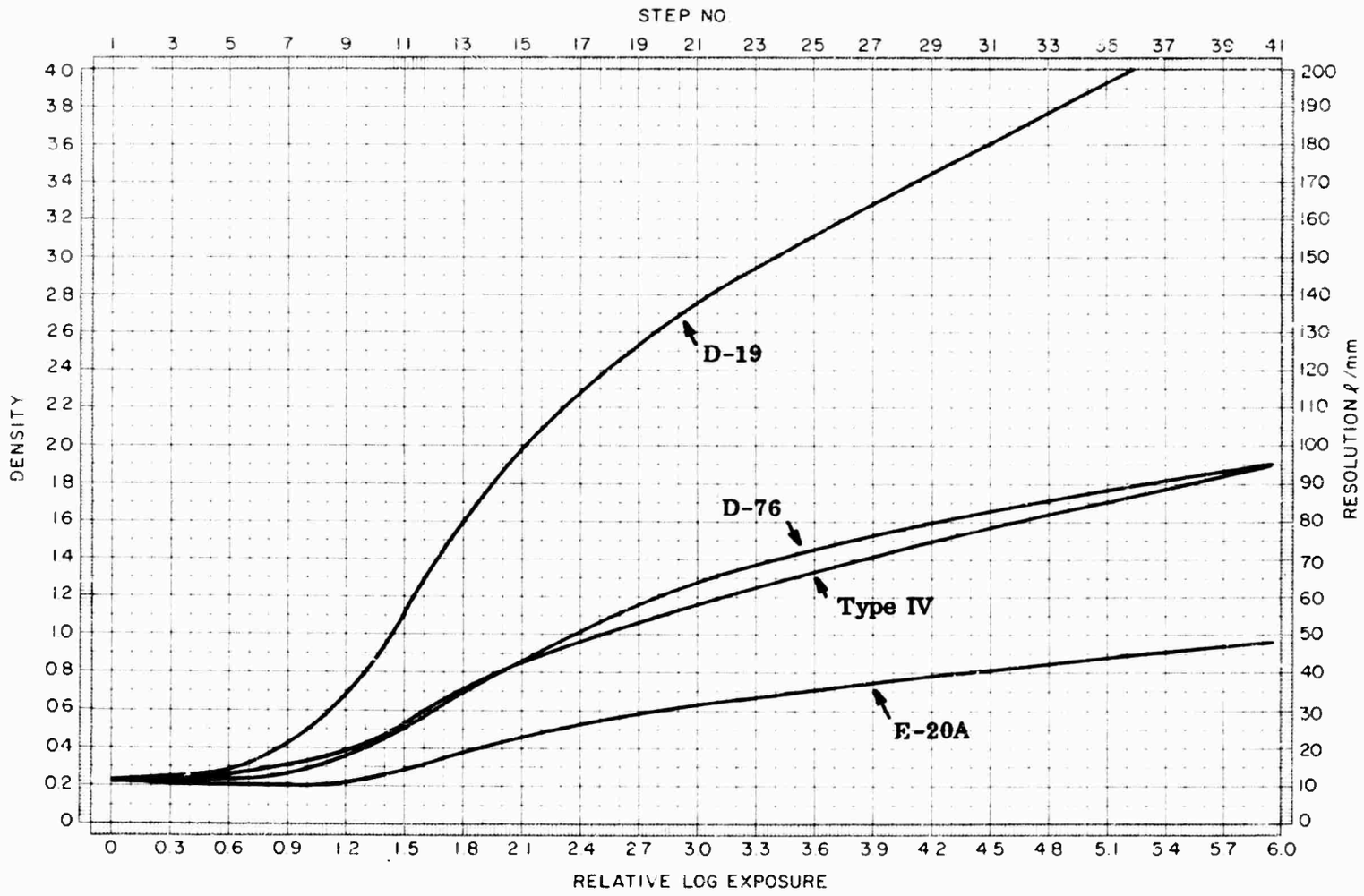

Figure 3. Characteristic Curves for Plus-X, Developed in D-19, D-76 (1:1), XDR Type IV, and XDR E-20A

EXTENDED RANGE PAPER

67

Plus-X
EK

10

4m 70

10

tech ops

TECHNICAL OPERATIONS
CORPORATED
BURLINGTON, MASSACHUSETTS

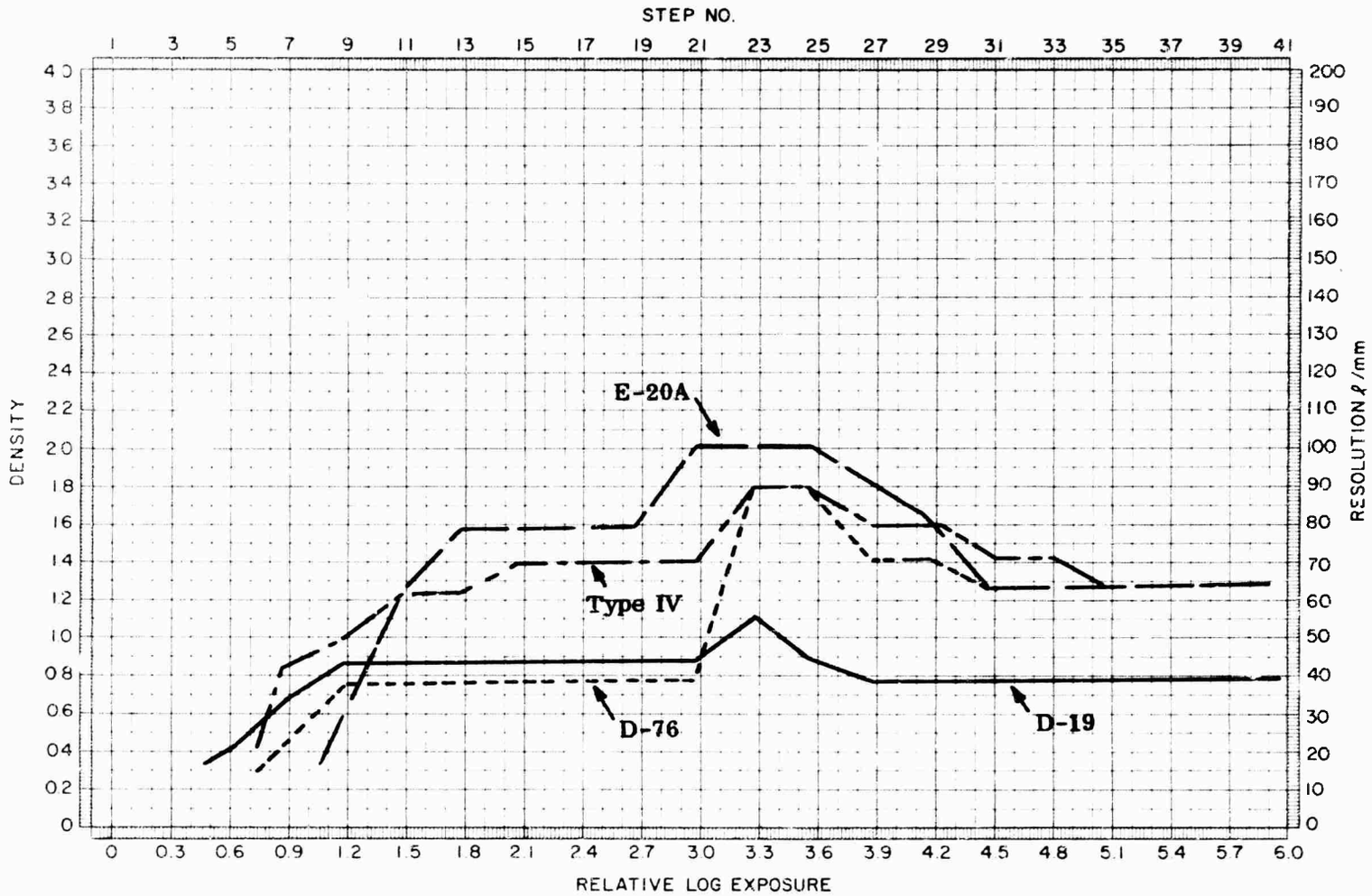

Figure 4. Resolution Curves for Plus-X, Developed in D-19, D-76 (1:1), XDR Type IV, and XDR E-20A

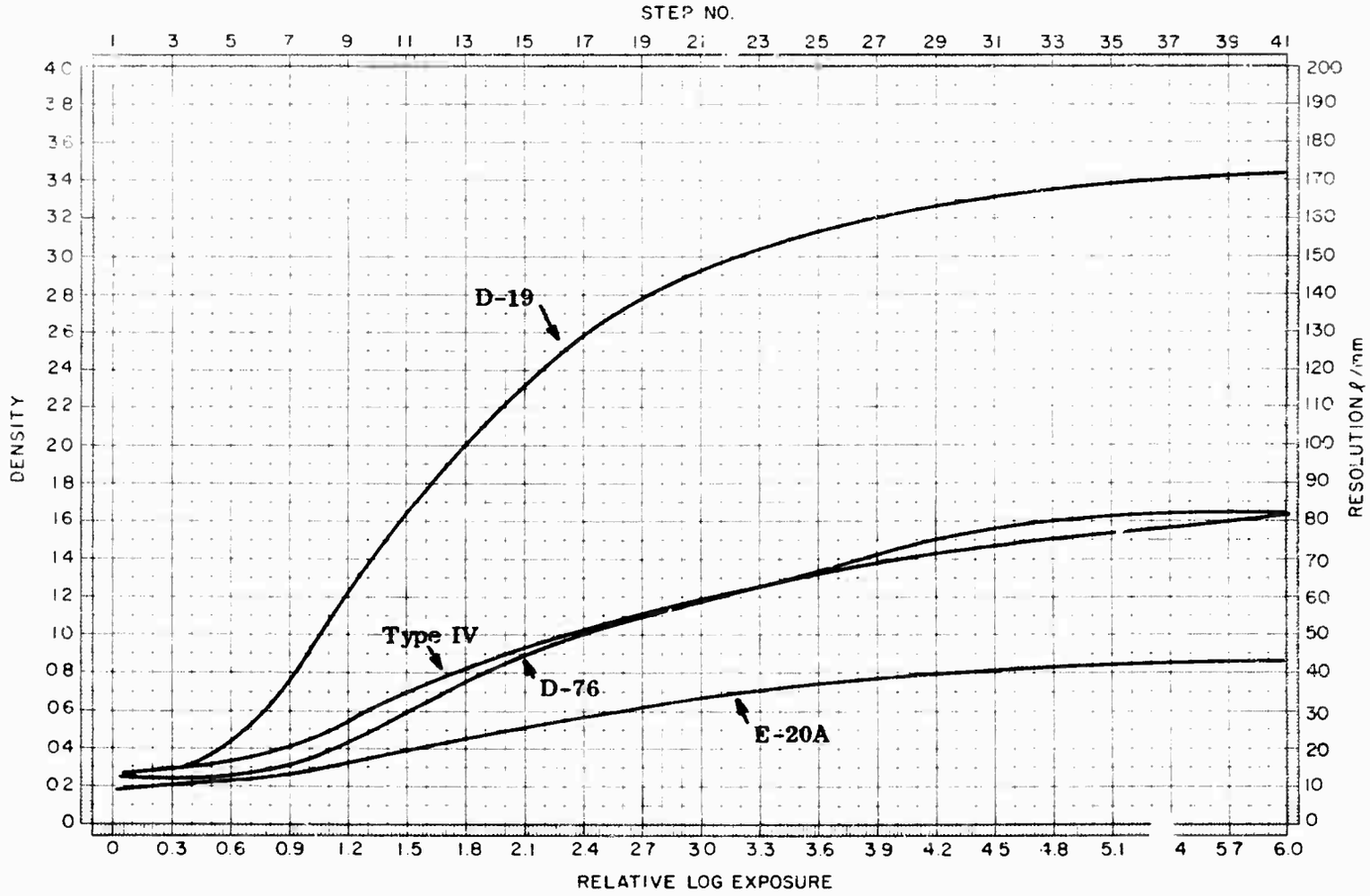

Figure 5. Characteristic Curves for Tri-X, Developed in D-19, D-76 (1:1), XDR Type IV, and XDR E-20A

EXPANDED RANGE PAPER

DATE 67

PROCESSED BY

TYPE Tri-X

MANUFACTURER EK

SENSITOMETER

EXPOSURE TIME 10 SEC.

DEVELOPER

DEVELOPING 4m AT 70 °F

DEVELOPMENT CONDITIONS

SENSITOMETRIC PROPERTIES

BASE DENSITY

SPEED AT D =

GAMMA

ABS LOG E

12

TECHNICAL OPERATIONS, INCORPORATED
BURLINGTON, MASSACHUSETTS

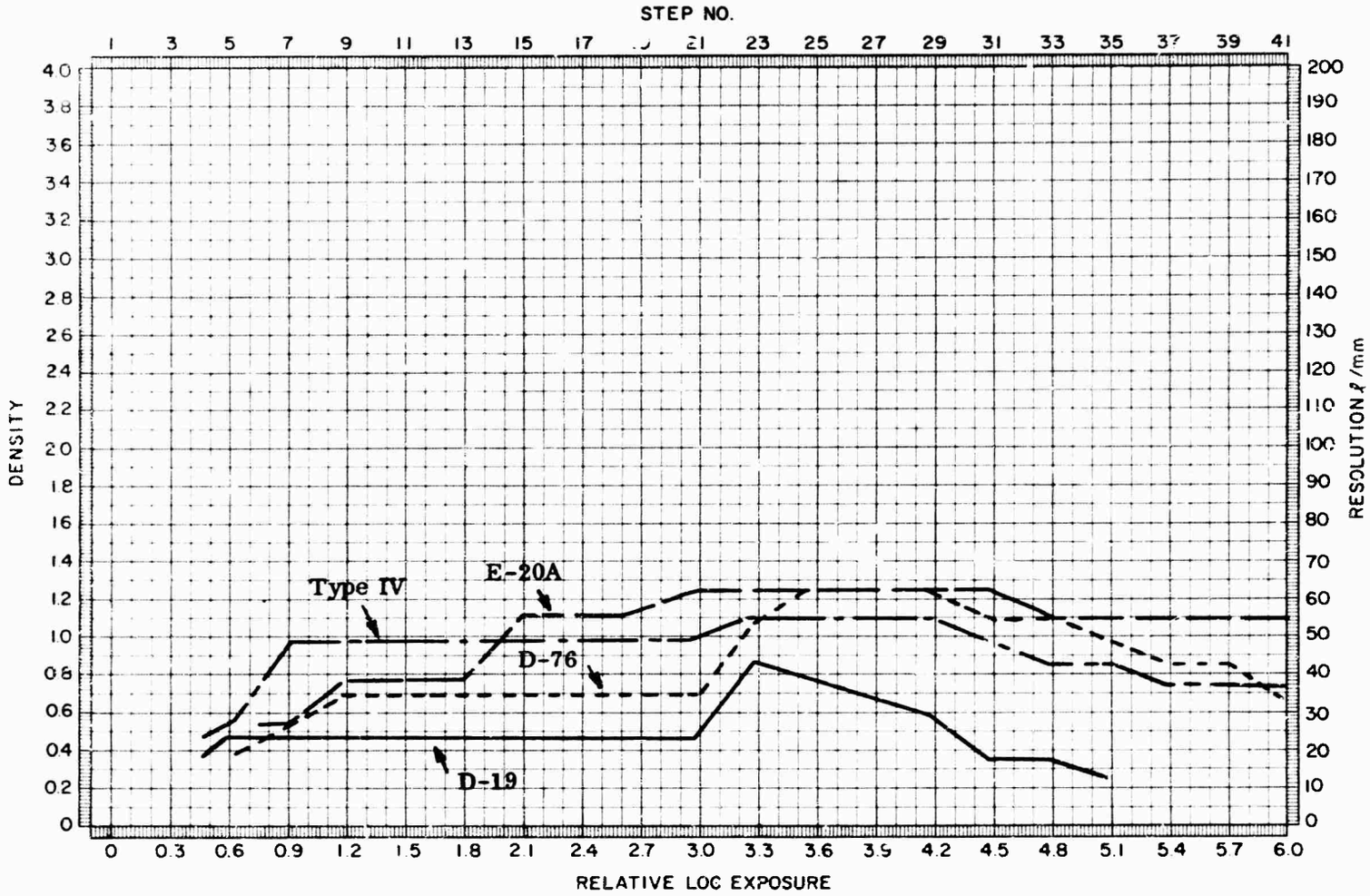

Figure 6. Resolution Curves for Tri-X, Developed in D-19, D-76 (1:1), XDR Type IV, and XDR E-20A

Of particular interest is High Speed IR film, whose curves are shown in Figures 7 and 8. Observe that D-19 shows a very narrow exposure latitude and moderately low resolution values; yet this developer is generally used for this film because of its high toe speed, as seen in Figure 7 (to be discussed below). Of the other developers, D-76 appears to show good range compared to Type IV and E-20B (note the curve for E-20A is too slow for use with this film, and so data for E-20B are given—see Table I). However, the resolution data of Figure 8 show superior peak resolution and width of resolution for the two XDR developers.

SUMMARY OF DATA

Of considerable interest to experimentalists is the effect of new developers on film speed or sensitivity. These effects are best observed by direct field test or by examination of the characteristic curves. However, a speed point, S, can be calculated that is similar to the ASA speed criterion:

$$S = 1/E \text{ (mcsec at } D = 0.1 + \text{fog)}$$

(in the ASA convention, $S = 0.8/E$, where E is in mcsec at 0.1 above fog, but under stringent conditions of developer and developed contrast). These speed values are tabulated for the films studied in Table II and are plotted as a function of developer type in Figure 9a. These values indicate that D-19 always shows the highest toe speeds, that E-20A (or E-20B) shows low speeds, while Type IV speeds are just lower than those of D-76. Field tests will show if these lower toe speeds cause lower detectivity in the low-exposure region, or if they are detrimental to the recording of information in well-exposed areas.

The peak resolution values for the films studied are also tabulated in Table II and presented in Figure 9b. The resolution superiority of the XDR developer for the faster films (except Pan-X) is apparent from Figure 9b.

The standard sensitometric parameters of density (D_{max}) and gamma are presented in Table II and in Figures 10a and 10b. The lower values of density and gamma, obtained with the XDR developers, are related, we believe, to the lower granularity and high detectivity obtained with these developers.

Extended Range Resolution

Of special interest to us is our observation that the use of XDR developers on films broadens the log E range over which they show detectivity. One way to demonstrate this is to tabulate from Figure 2, 4, 6, and 8 the log E range over which some arbitrary resolution value is held. This is done in Table II at 80 lines/mm, 70 ℓ/mm, 40 ℓ/mm, and 40 ℓ/mm for Pan-X, Plus-X, Tri-X, and IR films, respectively. The tabulated log E values are plotted in Figure 11a, and they show that the XDR developers can exhibit a Δ log E range of 0.6 to 2.0 greater than that of D-76 and a still greater advantage over D-19. We believe that Figure 11a is of significant interest.

A calculation of similar interest, but less easy to interpret, is that of Δ log E shown by the film between the fog level and an arbitrary D_{max}. We base this calculation on the fact that granularity increases with D, and that resolution decreases with D. Therefore, those developers that allow a film to show an increase of density with exposure (dD/d log E) without reaching a high D_{max} (as the XDR developers do) should

67

High-Speed Infrared
EK

10

4m 70

7.10-10

TECHNICAL OPERATIONS,
INCORPORATED
BURLINGTON, MASSACHUSETTS

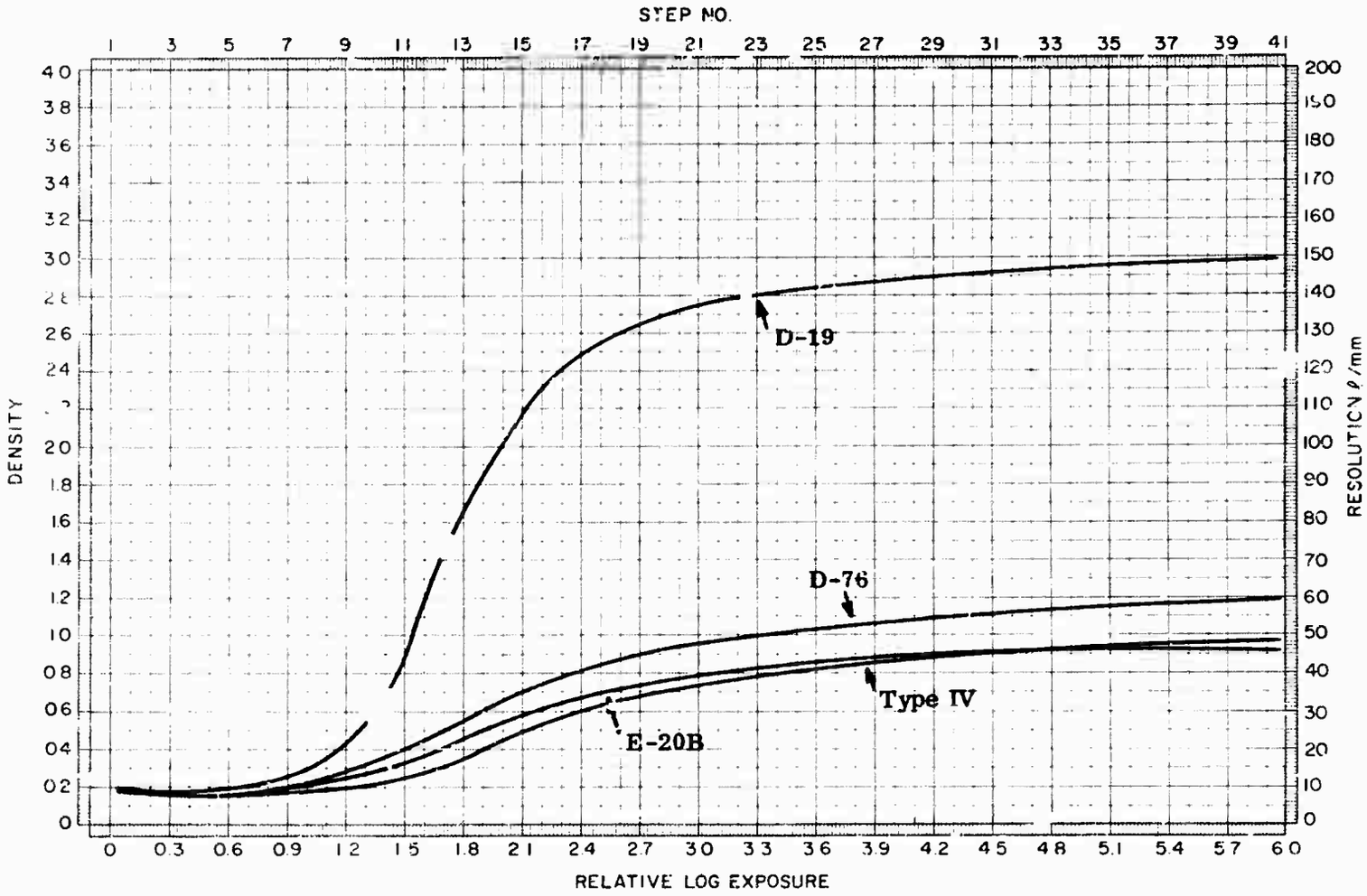

Figure 7. Characteristic Curves for High-Speed Infrared, Developed in D-19, D-76 (1:1), XDR Type IV, and XDR E-20B

EXTENDED RANGE PAPER

DATE 67

TYPE High-Speed Infrared

MANUFACTURER EK

EXPOSURE TIME 10 SEC.

DEVELOPER

DEVELOPMENT 4m AT 70°F

DEVELOPMENT CONDITIONS

SENSITOMETRIC PROPERTIES

BASE DENSITY

SPEED AT D

GAMMA

ABS LOG E

TECHNICAL OPERATIONS,
INCORPORATED
BURLINGTON, MASSACHUSETTS

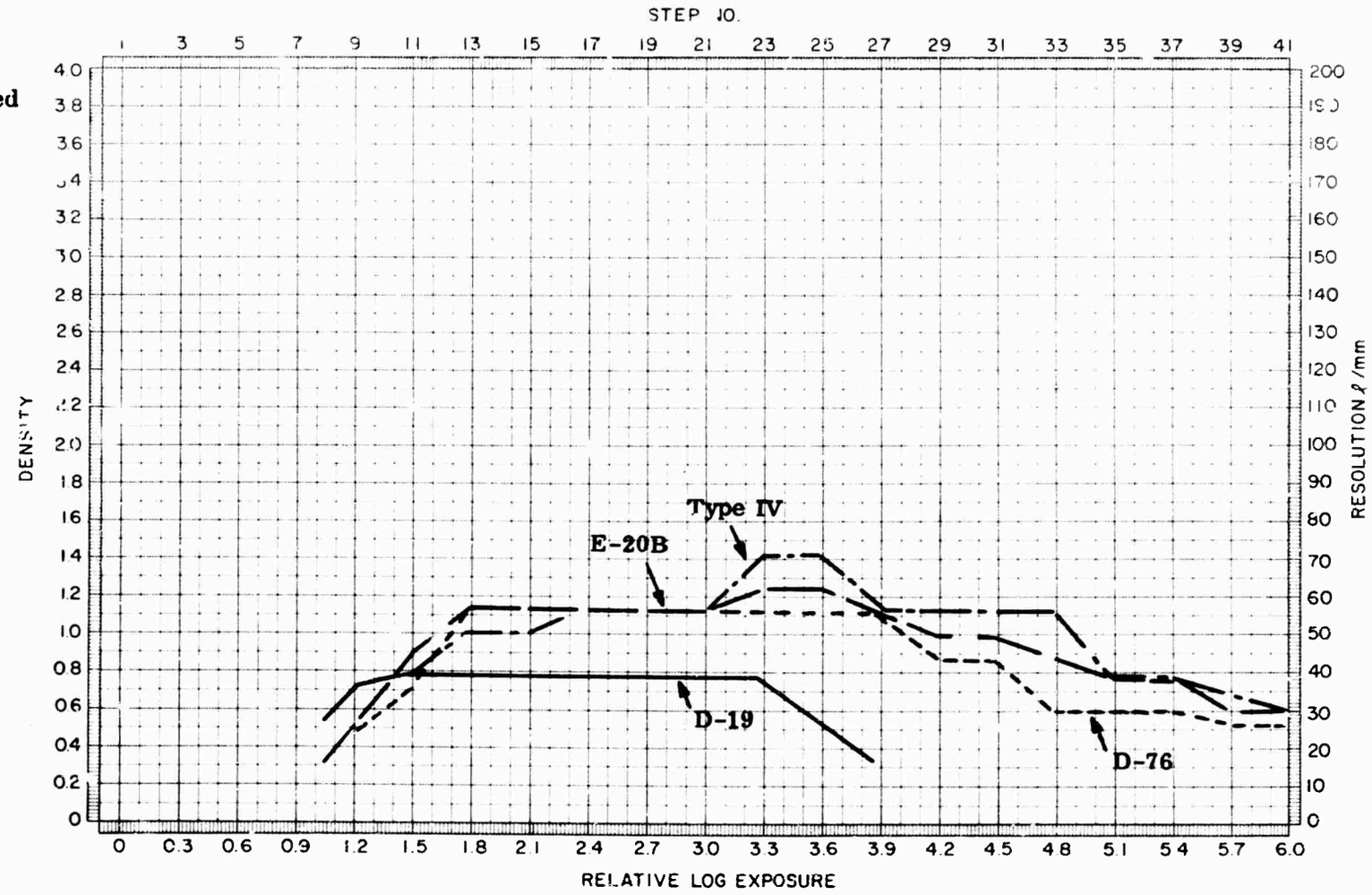

Figure 8. Resolution Curves for High-Speed Infrared, Developed in D-19, D-76 (1:1), XDR Type IV, and XDR E-20B

TABLE II

SENSITOMETRIC XDRM RESULTS
(All sensitometry at 10 sec exposure, 125 mcsec unattenuated, .og E = 7.10-10)

Film	Developer		Toe Speed*	D_{max}	Peak Resolution† (ℓ/mm)	γ	Δ Log Exposure‡	
							at Resolution = 80 ℓ/mm	at ΔD = 1.5 - Fog
Pan-X	Control	D-19	70	3.40	104	1.36	2.2	1.3
		D-76	43	2.10	114	0.84	2.2	2.6
	T/O XDR	E-20A	35	1.30	114	0.33	3.7	3.4
		Type IV	29	1.70	114	0.49	3.8	5.2+
							at Resolution = 70 ℓ/mm	at ΔD = 1.5 - Fog
Plus-X	Control	D-19	140	4+	50	1.4	0	1.2
		D-76	66	2.2	70	0.64	1.1	3.1
	T/O XDR	E-20A	23	1.0	100	0.24	3.3	4.8+
		Type IV	80	1.95	80	0.52	2.2	3.9
							at Resolution = 40 ℓ/mm	at ΔD = 1.5 - Fog
Tri-X	Control	D-19	310	3.4	40	1.4	0.9	1.2
		D-76	160	1.9	55	0.7	2.5	3.2
	T/O XDR	E-20A	50	1.6	68	0.2	4.2+	4.6
		Type IV	130	0.9	55	0.4	4.5	4.2+
							at Resolution = 40 ℓ/mm	at ΔD = D_m - Fog
High Speed IR	Control	D-19	80	3.0	36	2.0	0	1.2 at D_m = 2.0
		D-76	50	1.2	55	0.5	2.9	5.1 at D_m = 1.2
	T/O XDR	E-20B	40	0.95	64	0.4	3.6	5.1 at D_m = .95
		Type IV	20	0.90	70	0.5	3.6	5.1 at D_m = .90

*S = 1/E (mcsec at 0.1 above fog)
†Maximum of resolution - log E curve
‡Δ log E on characteristic curve over ΔD value stated, or over resolution limit stated

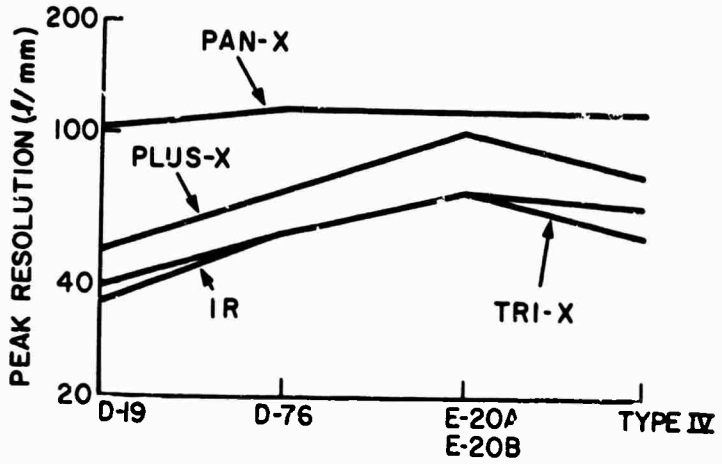

(a)

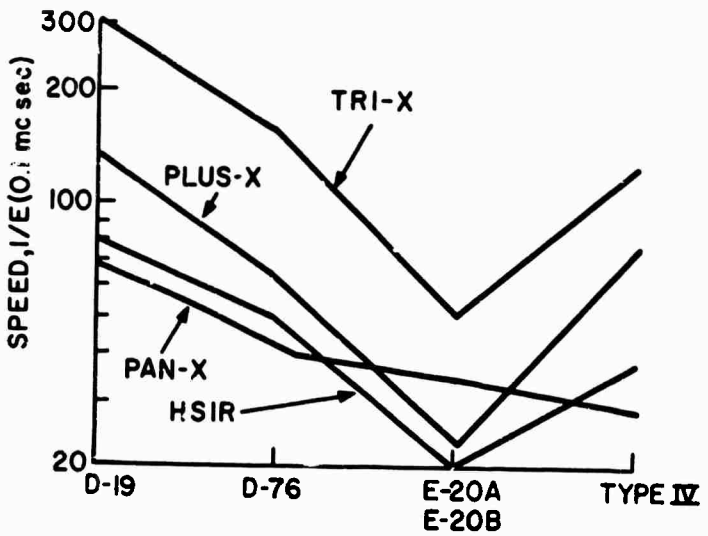

(b)

Figure 9. Speed-Resolution Data for Four Films Processed in Control and XDR Developers

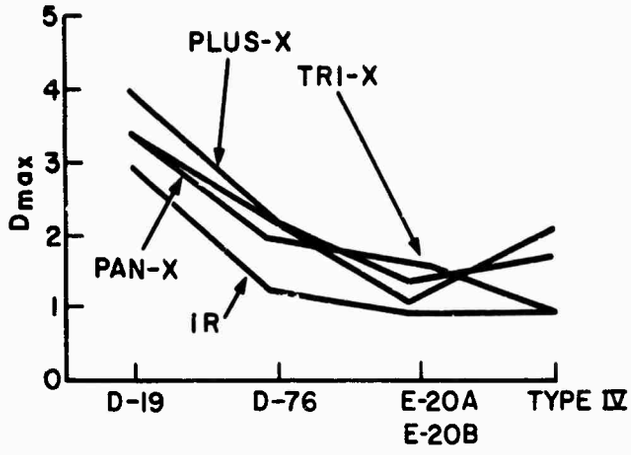

(a)

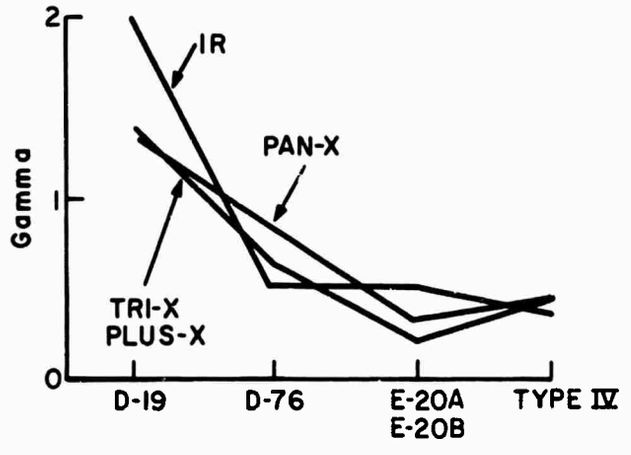

(b)

Figure 10. Density-Gamma Data for Four Films Processed in Control and XDR Developers

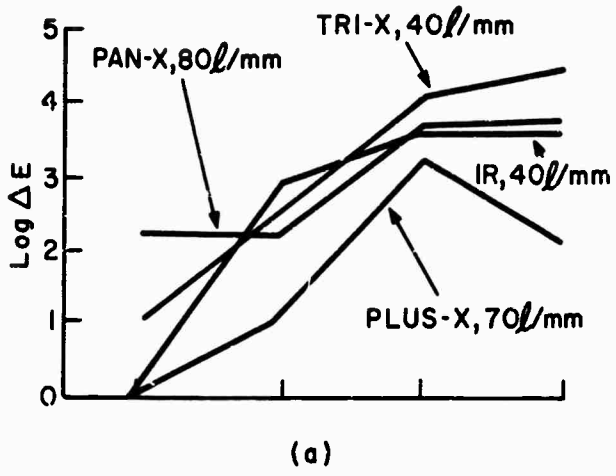

(a)

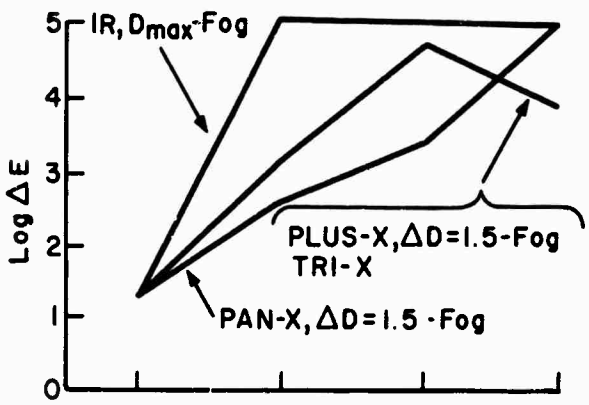

(b)

Figure 11. Dynamic Range Data for Four Films Processed in Control and XDR Developers

exhibit higher resolution and detectivity than those developers that quickly drive a film to a high D_{max}. These Δ log E values for Pan-X, Plus-X, and Tri-X calculated for $\Delta D = 1.5$ - fog are shown in Table II and are plotted in Figure 11b. The broader range of the XDR developers is clearly shown in these data. The case for High Speed IR is different. The D-19 curve quickly reaches a high value and so we compute $\Delta \log E$ for $\Delta D = 2.0$ - fog, and we obtain the low value of 1.2. Developer D-76, E-20B, and Type IV only reach low densities (Table II) and so we compute $\Delta \log E = 5.1$ in all three cases for $\Delta D = D_{max}$ - fog.

CONCLUSION

This concludes the sensitometric-resolution studies performed on this program. On the related program,[2] a great deal of sensitometry through filters and at various exposure times was performed, and figures of merit relating sensitivity and resolution were derived and calculated that are of importance in wide exposure-latitude photography. This sensitometric and resolution work of both programs established the wide latitude and extended dynamic range capability of the XDR developers. It then remained to study the specific extended range and flare-removal properties of these developers.

SECTION III

GRANULARITY AND DETECTIVITY

We believe that much of the success of XDR developers in reducing flare and increasing detectivity is due to the lower granularity of images processed in XDR developers. This will become apparent in our presentation of photomicrographs and microdensitometer traces of developed slit images in Section IV. This will also explain how the lower density and gamma scale of the XDR developers can actually increase the detectivity in overexposed images. Since this reasoning depends on an understanding of granularity and detectivity theory, we wish to present these ideas as an introduction to our experimental flare studies.

GRANULARITY

If a uniformly exposed and developed film is probed with an incident light of intensity I_o, and if the transmitted light is I, then the transmittance, T, is defined as;

$$T = I/I_o \tag{1}$$

while the density D is defined as

$$D = -\log T = \log (1/T) = \log (I_o/I) \ . \tag{2}$$

In both expressions (1) and (2), it is assumed that the area over which I_o is presented to the film is large enough to cover a statistical sample of film grains and that T and D will be constant over the uniformly exposed film. In practice, the scanning area in an ASA diffuse-density reading is about 1/16 in. = 1500 μ, an area large enough to include some 10^6 grains.

Now let the probing aperture A become quite small: 10-200 μ. Then the T and D values read through it will fluctuate with the location of the aperture on the film. If we let the aperture scan over the film in a linear dimension x, then a trace of T (x, A) is created, as in Figure 12. The root-mean-square average of the transmittance, $\sigma(\overline{T}, A)$, may be defined[4-6] as an integral

$$\sigma^2 (\overline{T}, A) = \frac{1}{A} \int (T(x) - \overline{T})^2 \, dA \tag{3}$$

or as a sum

$$\sigma^2 (\overline{T}, A) = \frac{1}{n} \sum_{1}^{n} (\overline{T}(x) - T)^2 \ . \tag{4}$$

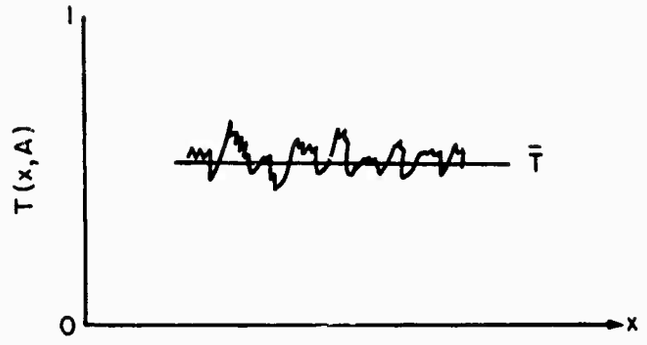

Figure 12. Transmittance Trace with Aperture A

In photographic work, we deal mostly with density, and for small fluctuations we find that:

$$dD = -0.43 \ln (1 - dT/\bar{T})$$

$$(D, A) = \frac{0.43\, \sigma(T, A)}{\bar{T}} \quad . \tag{5}$$

Because of Eq. (5) it is customary to speak in terms of $\sigma(D, A)$ rather than in terms of $\sigma(T, A)$, which is harder to measure. The granularity of developed film is defined as $\sigma(D, A)$:

$$\sigma^2(D, A) = \frac{1}{n} \sum_{1}^{n} (\bar{D} - D)^2 \tag{6}$$

that is, as the root-mean-square fluctuations of the density, at average density $\bar{D}$, using a scanning aperture A. It has been found experimentally[6] that at constant $\bar{D}$, $\sigma(D, A)$ varies as $1/\sqrt{A}$, and this leads to the definition of Selwyn Granularity

$$SG = \sqrt{A}\, \sigma(D) \ , \tag{7}$$

where SG is independent of A.

Measurement of Granularity

To measure granularity, one must first generate a trace of D(x, A) or T(x, A) versus x, as in Figure 12, using a microdensitometer. The computation of $\sigma(D, A)$ by Eq. (6) is difficult if done by hand, since 1000 points are needed to give a good sample, and since $(\bar{D})$ must not vary appreciably during the run. This is best done by recording the D(x, A) trace on tape and feeding the tape into a computer in which $\sigma(D, A)$ is calculated by Eq. (6). In a more sophisticated approach, the D(x, A)

trace is used to compute the autocorrelation function and/or the Weiner power spectrum of the trace, from which $\sigma(D, A)$ is then computed. All these computer operations are being worked out in our own laboratory, but at this time we cannot present computed granularity data.

However, an indication of $\sigma(D, A)$ can be obtained directly by observation of the trace of D(x, A). By definition, σ is the rms value of the trace, and, therefore, the width of the trace is an indication of the granularity. This is the qualitative criterion of the granularity that we shall use in the slit analysis below.

DETECTIVITY OR SENSITIVITY

Let us see how the detectivity of a film is limited by its granularity. In photographic work one often uses the term "sensitivity" to mean the reciprocal of the minimum energy needed to detect a first signal, i.e., speed, as in Eq. (1). But in detection theory, sensitivity or detectivity often means the ability to discriminate a small signal in the presence of a background, or a small signal increment over a strong signal.[7] Let this detectivity be d (S for sensitivity in Zweig's notation)[7]:

$$d = \frac{1}{\Delta E^{*}(D, A)} \tag{8}$$

where ΔE^{*} is the minimum exposure difference that can be recorded on the film at density D on area A. To compute d, let us sketch an ideal characteristic curve as in Figure 13, in which the horizontal coordinate is E (exposure units) rather than log E. Then the slope of the curve is g, and the limiting detectable energy is given by:

$$\Delta E^{*} = \Delta D^{*}/g \ . \tag{9}$$

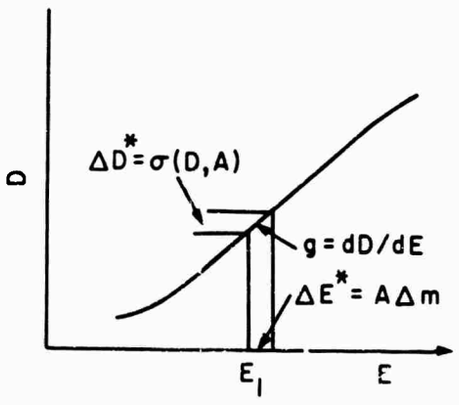

Figure 13. Ideal Detectivity Curves

From this the detectivity, d, is given by:

$$d = g/\Delta D^* \quad . \tag{10}$$

But g is a slope that depends on absolute exposure units, and it is best to express Eq. (10) in terms of the dimensionless γ:

$$\gamma = dD/d \log E = 2.3\ E_1\ g \tag{11}$$

where E_1 is the absolute exposure at the point at which g or γ is measured. From this, we obtain for d:

$$d = \gamma/2.3\ E_1\ \Delta D^* \quad . \tag{12}$$

From (12) it would appear that to increase detectivity, one should increase γ, but in addition there is the effect of ΔD^*. The key assumption in detection theory is that:

$$\Delta D^* = \sigma(D, A) \tag{13}$$

that is, the developed granularity of the film (at density D, and area of signal A) limits the detectivity. Then the final expression for d is given by Eq. (13):

$$d = \frac{\gamma}{2.3\ E_1\ \sigma(D, A)} \quad . \tag{14}$$

Equation (13) is quite important. The term in $(1/E_1)$ is essentially the "speed" of the film; thus, fast films are better detectors than slow films. The term in γ indicates that higher contrast gives higher detectivity, while the term in $1/\sigma$ (D, A) shows that the more granular a film, the lower its detectability. For films of constant $(1/E_1)$ value, the ratio γ/σ determines the detectivity. In this report, the XDR developers lower γ but also lower σ(D, A) compared to the control developers, so that γ/σ is increased. They also raise the value of detectivity.

SECTION IV

FLARE STUDIES

PROJECTION LAMP EXPOSURE

In the past two years, we have performed numerous experiments with XDR developers in our laboratory that have shown that these developers qualitatively reduce flare. A typical example of this effect is shown in Figure 14, two photographs of a clear glass projection bulb. Figure 14a is a best print made from a Plus-X negative developed in D-76 (1:1) for 4 min at 68°F, and Figure 14b is a best print made from an identical exposure, developed in Type IV for 4 min at 68°F. The increased detectivity and reduction of flare are obvious, but a quantitative analysis of a photograph as complex as that of Figure 14 would be quite difficult. Therefore, we decided to initiate a set of experiments using controlled slit-aperture exposures. Before presenting these data, however, we will summarize our qualitative ideas on the term "flare."

DEFINITION OF FLARE

An appearance of density peripheral to an overexposed image, especially when no specific cause for it can be assigned, is often called a "flare." Flare is not an absolute property; it exists in varying degrees and kinds. This is not surprising, since an optical image, in itself, is a rather diffuse concept, and so a deviation from it is also indefinite. Any useful definition of flare, therefore, must include this idea of uncertainty.

Two types of flare may be distinguished: lens flare and film flare. Lens flare (which is simpler than film flare) can be defined as any light deviated from its image-forming direction in passing through the lens by factors other than normal lens aberrations. Thus, the term "flare" has come to be reserved for stray light whose cause is indefinite, uncertain, or unknown. When a cause is identified, it is usually associated with the stray light, and the residual is regarded as flare.

Film flare is any deviation in optical density from that expected from the exposure, apart from the fluctuations due to the inherent granular nature of photographic emulsions. Here, too, an obvious imperfection in processing, or an artifact on the film big enough to identify, is recognized specifically and removed from the discussion of film flare. Again, a diffuse, subtle, and uncertain factor is responsible for film flare.

Assigning loss of image contrast either to an actual cause or to some vague origin is unavoidably ambiguous. For example, the fine-scale irregular fluctuations of density found on uniformly exposed film will be discussed below in terms of granularity, $\sigma(D, A)$, expressed as the mean fluctuation of density probed with an aperture of area A. Quantitative measurements of $\sigma(D, A)$, however, include all the fluctuations observed, without attributing them exclusively to grain. Until we have an acceptable theory of the fluctuations attributable to the grains themselves, we may not be able to measure flare by the measurement of $\sigma(D, A)$. This is of practical importance to the problem of flare reduction, since our microdensitometer analyses show that the XDR developers markedly reduce $\sigma(D, A)$, as well as D_{max} and γ, and we feel that this reduction in $\sigma(D, A)$ is largely responsible for the apparent edge enhancement and flare reduction accomplished by the XDR developer.

a. Best Print of Plus-X Negative Developed in D-76 (1:1) for 4 min at 68°F

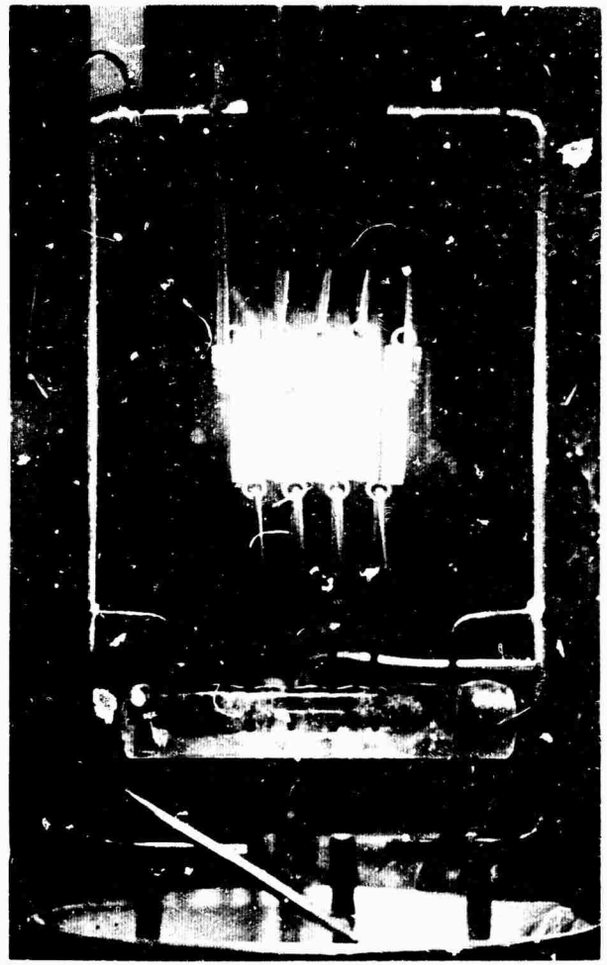

b. Best Print, Identical Exposure, Developed in Type IV for 4 min at 68°F

Figure 14. Example of Flare Reduction by XDR Developer

When a photographic film is only one part of a system, the flare found on the developed film will be a combination of the flares due to the various components of the system—a great complication in the practical investigation of film flare. Thus, the small angle scattering by minute bubbles in a lens, or local variations in the refractive index of the glass, will often be hard to distinguish from the scattering of the undeveloped emulsion.

With this qualitative discussion of flare, let us go on to a description of our controlled flare experiments.

FLARE EXPERIMENTS

Flare Exposure Method

Figure 15 shows a schematic of the optical bench imaging system used for all of our slit-width flare exposures that were subjected to various development treatments and microdensitometer analysis. The exposure object was a razor blade slit, imaged through a lens system operating at f/130. The two imaging lenses form a telescope with unit magnification, and the slit dimensions on the film plan were 1.7 x 14 mm.

The aperture in the spatial frequency plane, diameter 0.120 in., determines the frequency response of the imaging system. Because the focal ratio is f/130 and the aperture is small, the imaging system is diffraction-limited, with a resolution limit of about 10 lines/mm. The slit object was illuminated by a mercury arc light source whose output passes through a 500 μ pinhole and, then, through a collimating lens with a 15 in. focal length. The coherence interval of the light illuminating the object is calculated to be 500 μ. Since this is several times the resolvable area in the object, the illumination can be considered to be essentially coherent for this experiment.

The optical system shown in Figure 15 has several advantages over a simple camera lens for the study of film flare, because it eliminates or reduces lens flare to a negligible amount. The light transmitted directly through the object is brought to a focus in the spatial frequency plane; therefore, the aperture in this plane can be stopped down considerably without lowering the intensity in the image. This small aperture, in turn, reduces the lens flare by preventing any stray light that is reflected from the lens from reaching the film plane. Thus, lens flare can come only from the second imaging lens, and this flare, moreover, is held to a minimum because the lens is placed 15 in. from the film plane and it is an achromatic doublet with only two

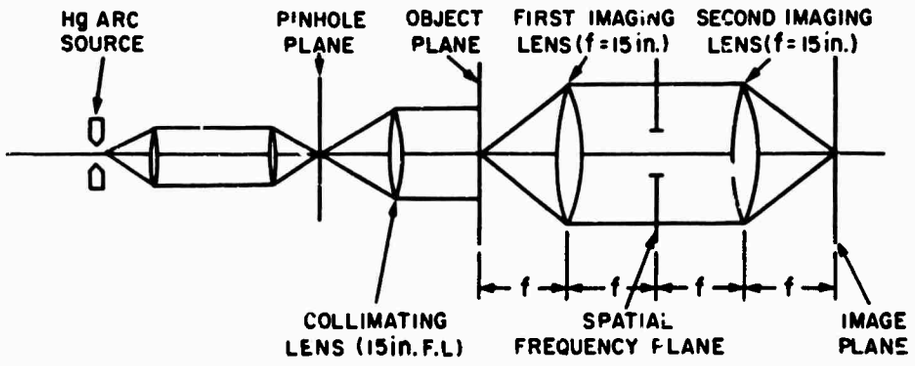

Figure 15. Optical Bench Imaging System

air-glass surfaces. In addition, because the imaging system works very nearly on-axis at a small aperture, lens vignetting is eliminated. The flare effects on the film, therefore, are due primarily to scattering effects associated with the film, and to development effects associated with high densities produced in the flare region.

Films were exposed to the slit image in a lensless Exacta camera body at an exposure time of 1 sec. The unattenuated light intensity of the slit source was approximately 10 times greater than that of the sensitometer, or about 12,500 metercandles.

Exposure Sequence

A given exposure sequence on any one film strip consisted of a series of thirteen exposures, covering four orders of attenuation, established by neutral density filters according to the following sequence:

ND = 0, 0.3, 0.6, 1.0, 1.3, 1.6, 2.0, 2.3, 2.6, 3.0, 3.3. 3.6, 4.0 .

For each film type, the slit sequences were shot through Wratten filters according to the following sequences:

Pan-X, Plus-X, Tri-X; 47 (blue), 12 (yellow), 25 (red)

High Speed IR; 47, 12, 89B (infrared).

Finally, each sequence was repeated in triplicate to allow for processing in three developers: D-19, E-20A, (E-20B for IR), and Type IV.

The widths of all developed slit images were measured with an 8X reticle magnifier. Next, all developed slit images were traced on a Joyce-Loebl microdensitometer at a linear magnification of 50:1 (so that the 1.7 mm slit width became 8.5 on the chart) and at scanning apertures of 10 μ and 5 μ.

Figure 16 shows a transmission photograph of part of a set of slit images. Figure 16a is High Speed IR film exposed through an 89B filter and developed in D-19, and Figure 16b is a photograph of the same exposure sequence developed in E-20B. The line broadening of the images developed in D-19 is apparent even from the unmagnified photograph of Figure 16.

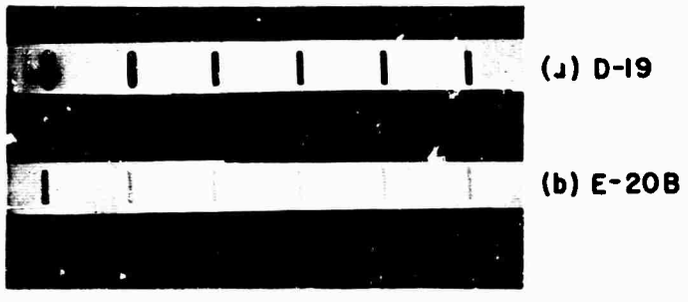

Figure 16. Comparison of Photomicrographs of Slit Images, High-Speed Infrared Film, 89B Filter, Developed in D-19 and Type IV

Low-Power Measurements

In the low-power set of measurements, we sought to determine if the XDR development of slit images would allow the slit widths to be more accurately measured on a comparator than those developed in D-19. This measurement would simulate the measurement of objects or spectral lines in a field application. Figure 17 shows photomicrographs at 30X of High Speed IR film taken through an 89B (infrared) filter at 0.6 ND and at 2.3 ND attenuation, developed in D-19 and in Type IV. In the D-19 images (17a and c), we note a uniform heavy density out to the edges, and flare density extending further out. In the Type IV development (17b and d), the main area of the slit is at low uniform density, and the edge is enhanced by an adjacency effect that makes the outer edge quite sharp.

Using a lower power (8X) comparator, we read the edge width of the slit images and plotted them in Figure 18 for High Speed Infrared film, exposed through an 89B filter and processed in D-19 and Type IV developers. The vertical scale is the linear dimension of the slit in millimeters, and the horizontal scale is Rel log E, on which the neutral density filters used to attenuate the exposure are superposed. Both developers show dimensions of 1.70 mm at maximum light attenuation of log E = 0 or ND = 4.0. At an exposure of log E = 4 (ND = 0), the Type IV developed edge is measured at 1.81 mm for an error of 6%. The two edges shown in the photomicrographs of Figure 17 are indicated in Figure 18 by arrows on the exposure scale at log E = 1.7 and 3.4, and the measured slit widths are 1.75 mm and 1.78 mm, respectively. The edges developed in D-19 flare out quite quickly. The two micrographs of Figure 17 show slit-width readings of 1.78 and 1.90 mm at log E = 1.7 and 3.4, respectively. At an exposure of log E = 4.0 (ND = 0), the D-19 slit is badly flared and its approximate width is read as 3.4 mm (100% error).

Figure 19 shows slit-width measurements for High Speed Infrared film exposed through a 47 filter in the region of blue sensitivity. The flare is much reduced in the blue, compared to the red region, an effect associated with the absorption of blue light in the depth of the grains, and absorptions of red light by the dyes on the surface of the grains. However, at high exposures, the flare of the D-19 slits is greater than that of the slits developed in Type IV (2.5 mm versus 1.80).

In Figures 20 and 21 we show slit-width exposure curves for Plus-X in red light (25 filter) and in blue light (47 filter) for development in D-19 and in Type IV. The behavior is similar to that for IR film. In red light, the D-19 flare is too great to be measured after log E = 3.6 (the value approaches 3.4 mm), while the maximum flare of the Type IV image is 1.82 mm, an error of only 8.5%. In Figure 21 for blue light, the effects are less striking, but Type IV gives the better values at high exposure.

Figures 22 and 23 show slit-width exposure curves for Tri-X film, using a 25 and a 47 filter, and the results are quite similar to those for Plus-X and Infrared film.

Microdensitometer (High-Power) Measurements

We have noted above that all the slit-width exposure sequences were traced on a Joyce-Loebl microdensitometer at an arm ratio of 50:1 (meaning that 1 mm on the film plane is spread out as 5 cm on the chart paper). The scanning aperture was 10 μ (equivalent on the film plane) for most measurements. It would not be practical or beneficial to present the entire microdensitometer analysis in this report. Therefore, we give in Figures 24, 25, and 26 the main results of this analysis, using High Speed

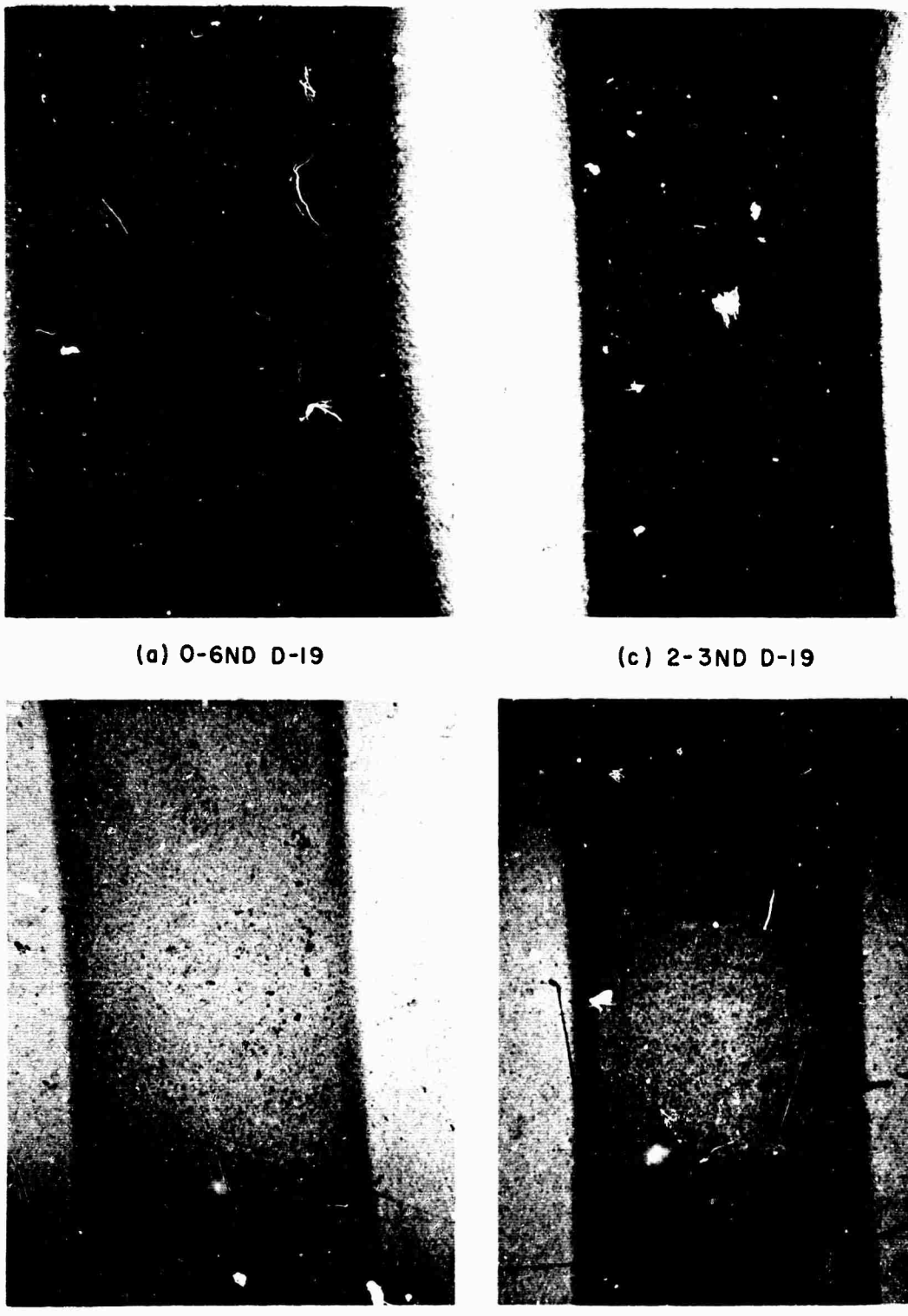

(a) 0-6ND D-19

(c) 2-3ND D-19

(b) 0-6ND TYPE IV

(d) 2-3ND TYPE IV

Figure 17. Photomicrographs of Slit Exposure of High-Speed Infrared Film, 89B Filter

Figure 18. Low-Magnification Slit-Width Measurement, High-Speed Infrared Film, 89B Filter

EXTENDED RANGE PAPER

DATE 10/6/67

PREPARED BY

FILM H.S. Infrared

MANUFACTURER

SENSITOMETER

EXPOSURE TIME SEC.

DEVELOPER

DEV. TIME AT °F

DEVELOPMENT CONDITIONS 89B Filter

SENSITOMETRIC PROPERTIES

BASE DENSITY

SPEED AT D =

GAMMA

ABS LOG E

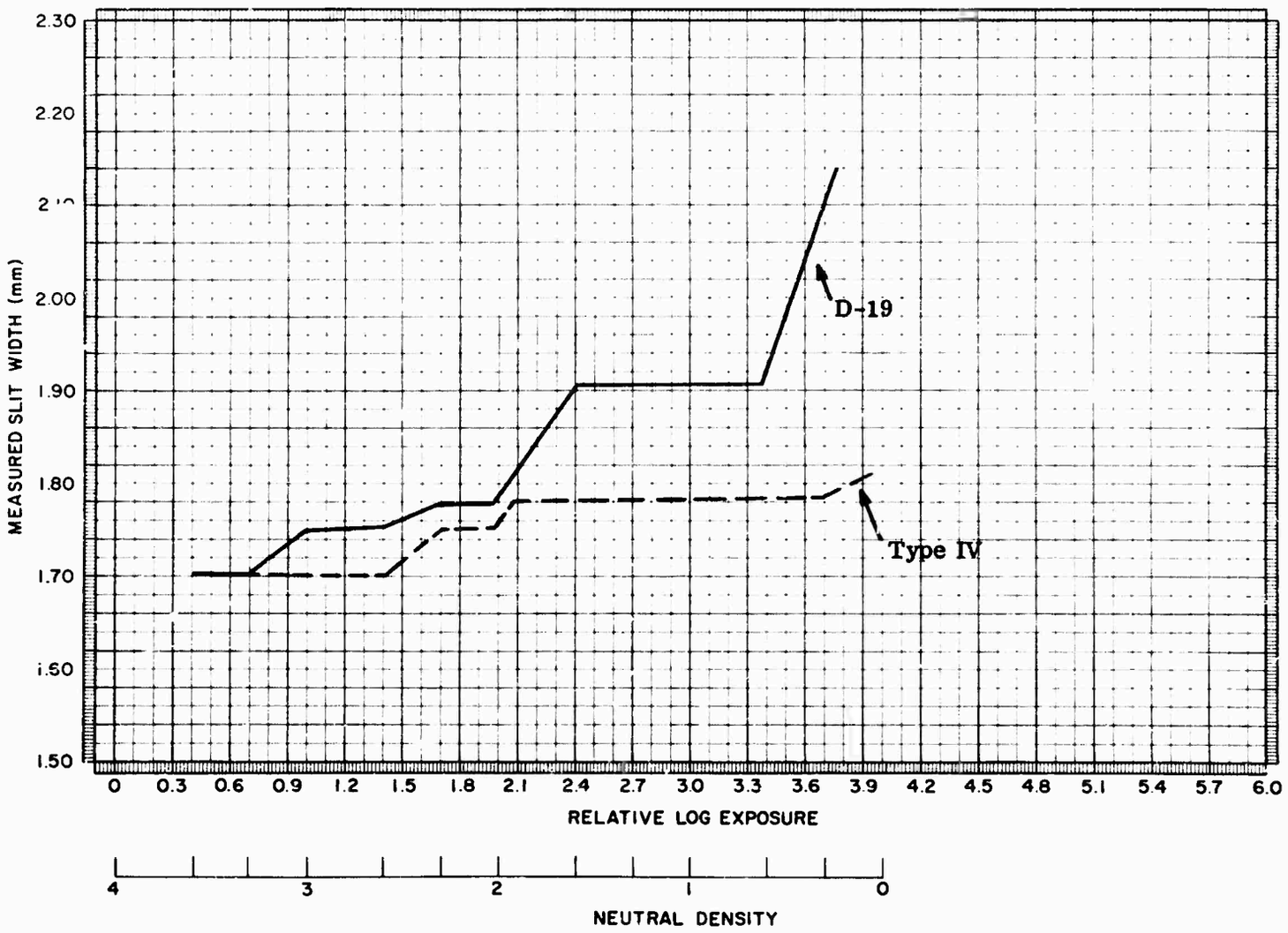

TECHNICAL OPERATIONS, INCORPORATED
BURLINGTON, MASSACHUSETTS

Figure 19. Low-Magnification Slit-Width Measurement, High-Speed Infrared Film, 47 Filter

EXTENDED RANGE PAPER

DATE 10/6/67

PREPARED BY

FILM H.S. Infrared

MANUFACTURER

SENSITOMETER

EXPOSURE TIME SEC.

DEVELOPER

DEV. TIME 4 min AT 68 °F

DEVELOPMENT CONDITIONS 47 Filter

SENSITOMETRIC PROPERTIES

BASE DENSITY

SPEED AT D =

GAMMA

ABS LOG E

tech ops
TECHNICAL OPERATIONS, INCORPORATED
BURLINGTON, MASSACHUSETTS

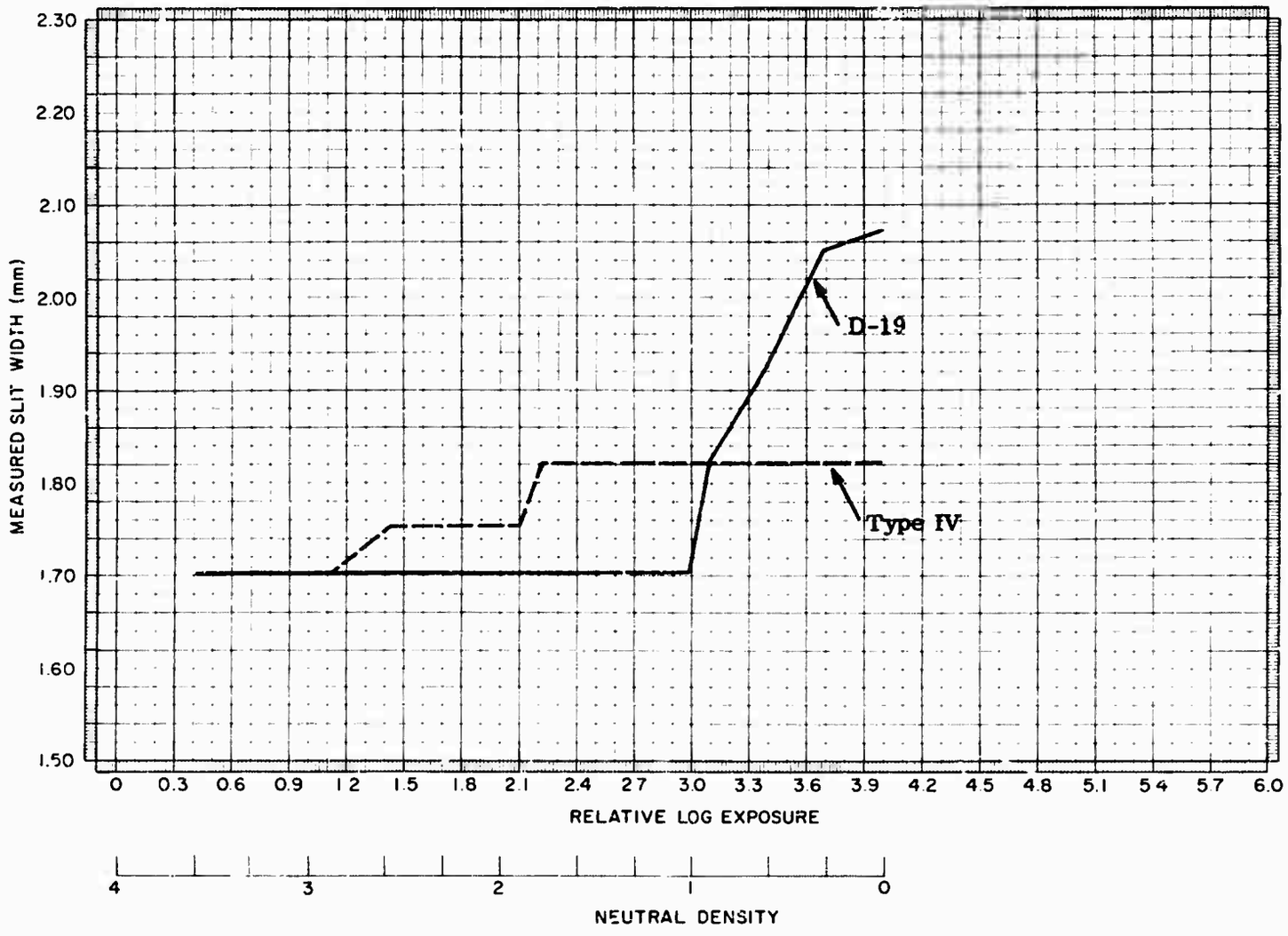

EXTENDED RANGE PAPER

DATE 10-6-67

PREPARED BY

FILM Plus-X

MANUFACTURER

SENSITOMETER

EXPOSURE TIME SEC.

DEVELOPER

DEV. TIME 4 min. AT 68 °F

DEVELOPMENT CONDITIONS 25 Filter

SENSITOMETRIC PROPERTIES

BASE DENSITY

SPEED AT D =

GAMMA

ABS LOG E

TECHNICAL OPERATIONS, INCORPORATED
BURLINGTON, MASSACHUSETTS

Figure 20. Low-Magnification Slit-Width Measurement, Plus-X Film, 25 Filter

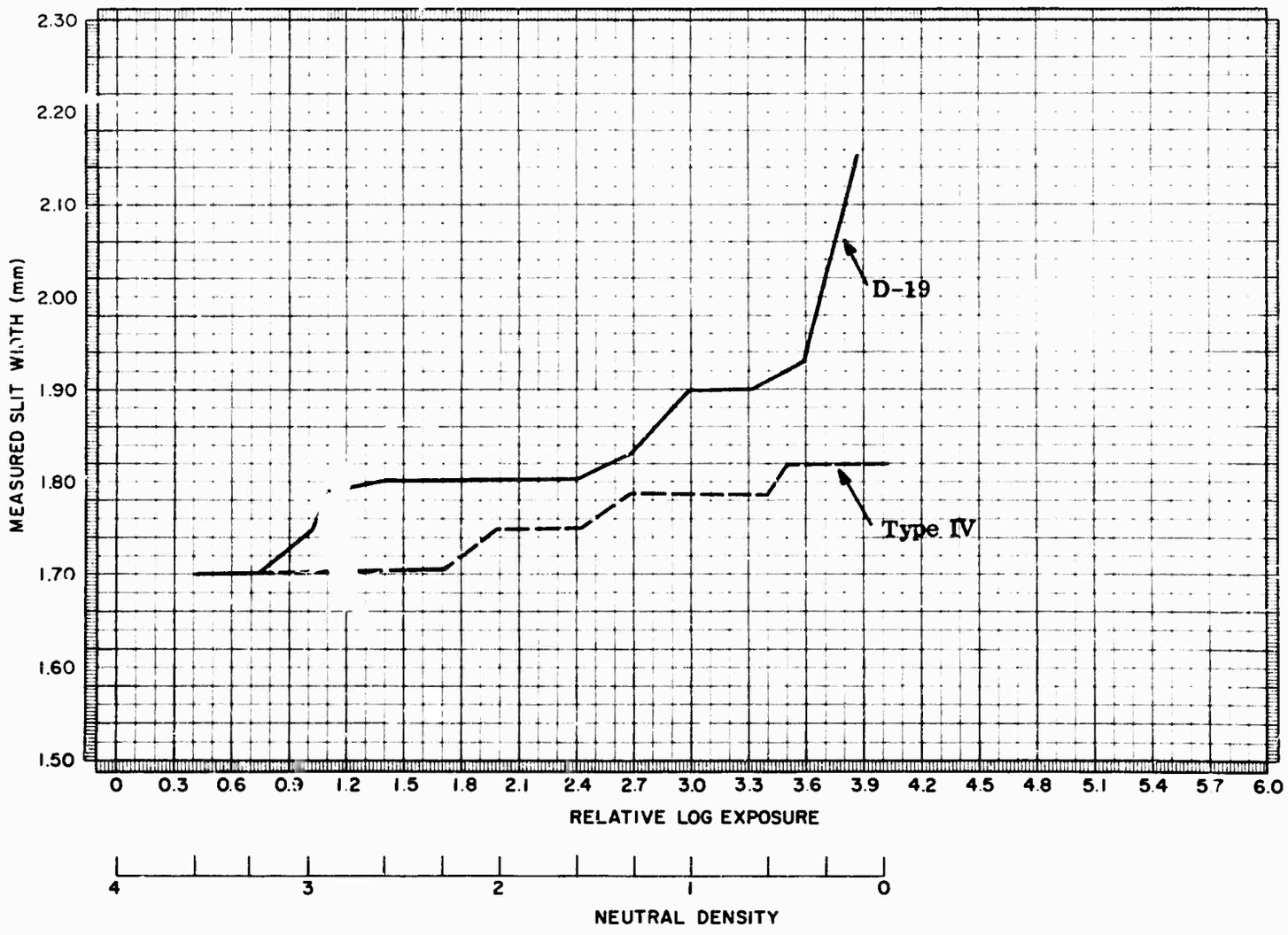

EXTENDED RANGE PAPER

DATE 10-6-67

PREPARED BY

FILM Plus-X

MANUFACTURER

SENSITOMETER

EXPOSURE TIME SEC

DEVELOPER

DEV. TIME 4 min 68 °F

DEVELOPMENT CONDITIONS 47 Filter

SENSITOMETRIC PROPERTIES

BASE DENSITY

SPEED AT D =

GAMMA

ABS LOG E

TECHNICAL OPERATIONS, INCORPORATED
BURLINGTON, MASSACHUSETTS

Figure 21. Low-Magnification Slit-Width Measurement, Plus-X Film, 47 Filter

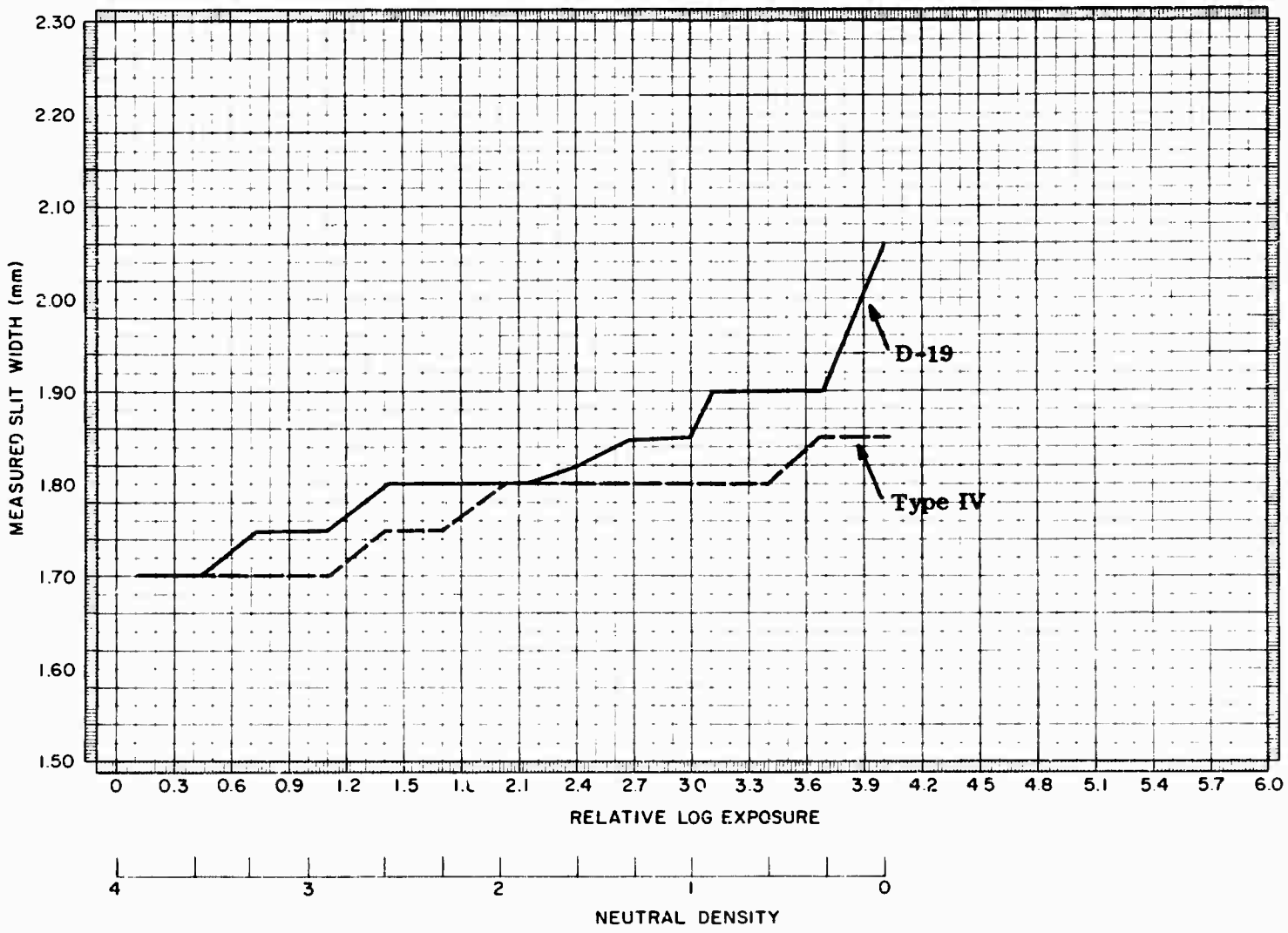

Figure 22. Low-Magnification Slit-Width Measurement, Tri-X Film, 25 Filter

EXTENDED RANGE PAPER

DATE 10-6-67

PREPARED BY

FILM Tri-X

MANUFACTURER

SENSITOMETER

EXPOSURE TIME SEC.

DEVELOPER

DEV. TIME 4 min AT 68 °F

DEVELOPMENT CONDITIONS 25 Filter

SENSITOMETRIC PROPERTIES

BASE DENSITY

SPEED AT D =

GAMMA

ABS LOG E

TECHNICAL OPERATIONS, INCORPORATED
BURLINGTON, MASSACHUSETTS

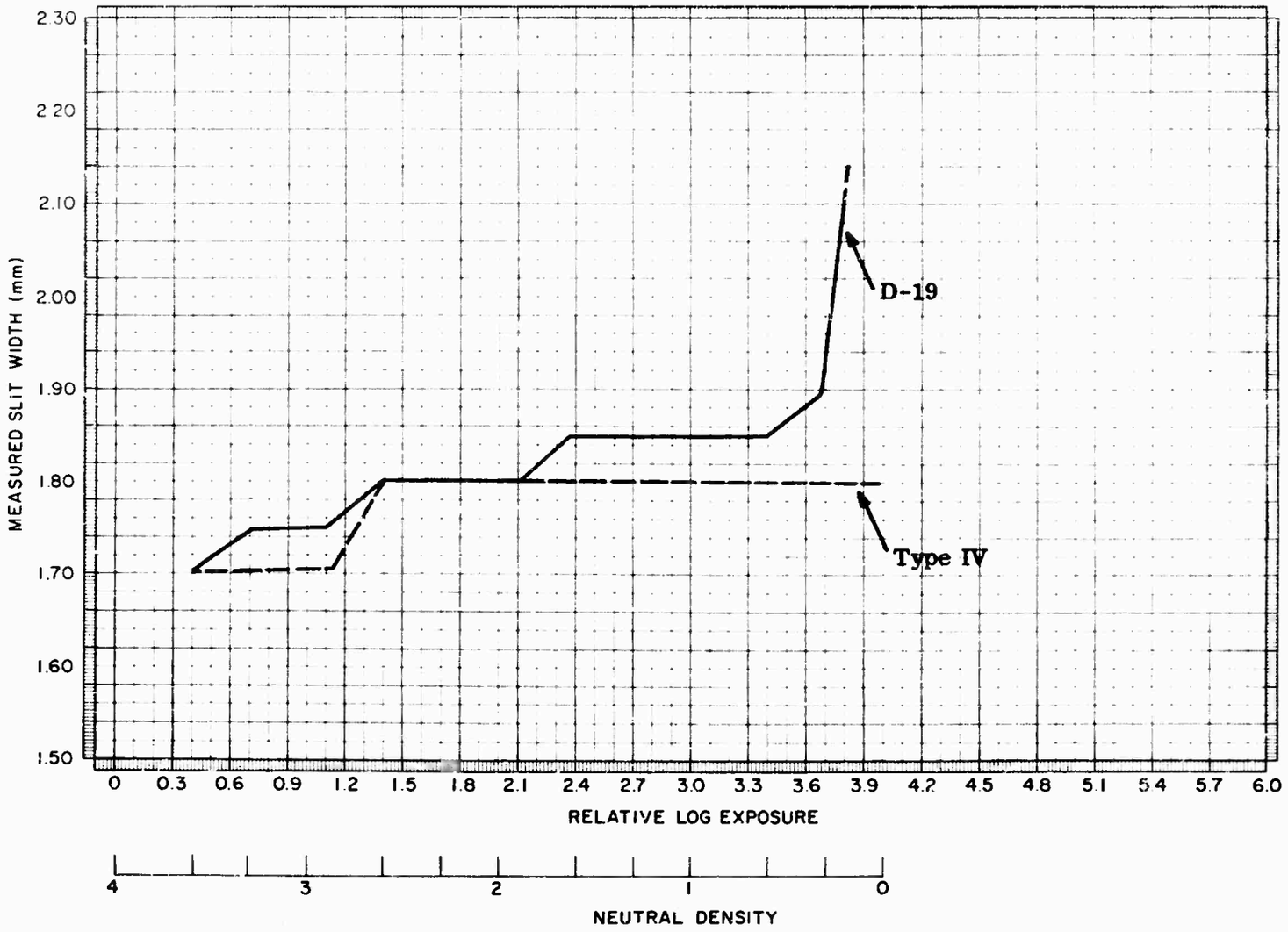

Figure 23. Low-Magnification Slit-Width Measurement, Tri-X Film, 47 Filter

EXTENDED RANGE PAPER

DATE 10-6-67
PREPARED BY
FILM Tri-X
MANUFACTURER

SENSITOMETER
EXPOSURE TIME SEC.
DEVELOPER
DEV. TIME 4 min AT 68 °F

DEVELOPMENT CONDITIONS 47 Filter

SENSITOMETRIC PROPERTIES

BASE DENSITY
SPEED AT D =
GAMMA

ABS LOG E

TECHNICAL OPERATIONS, INCORPORATED
BURLINGTON, MASSACHUSETTS

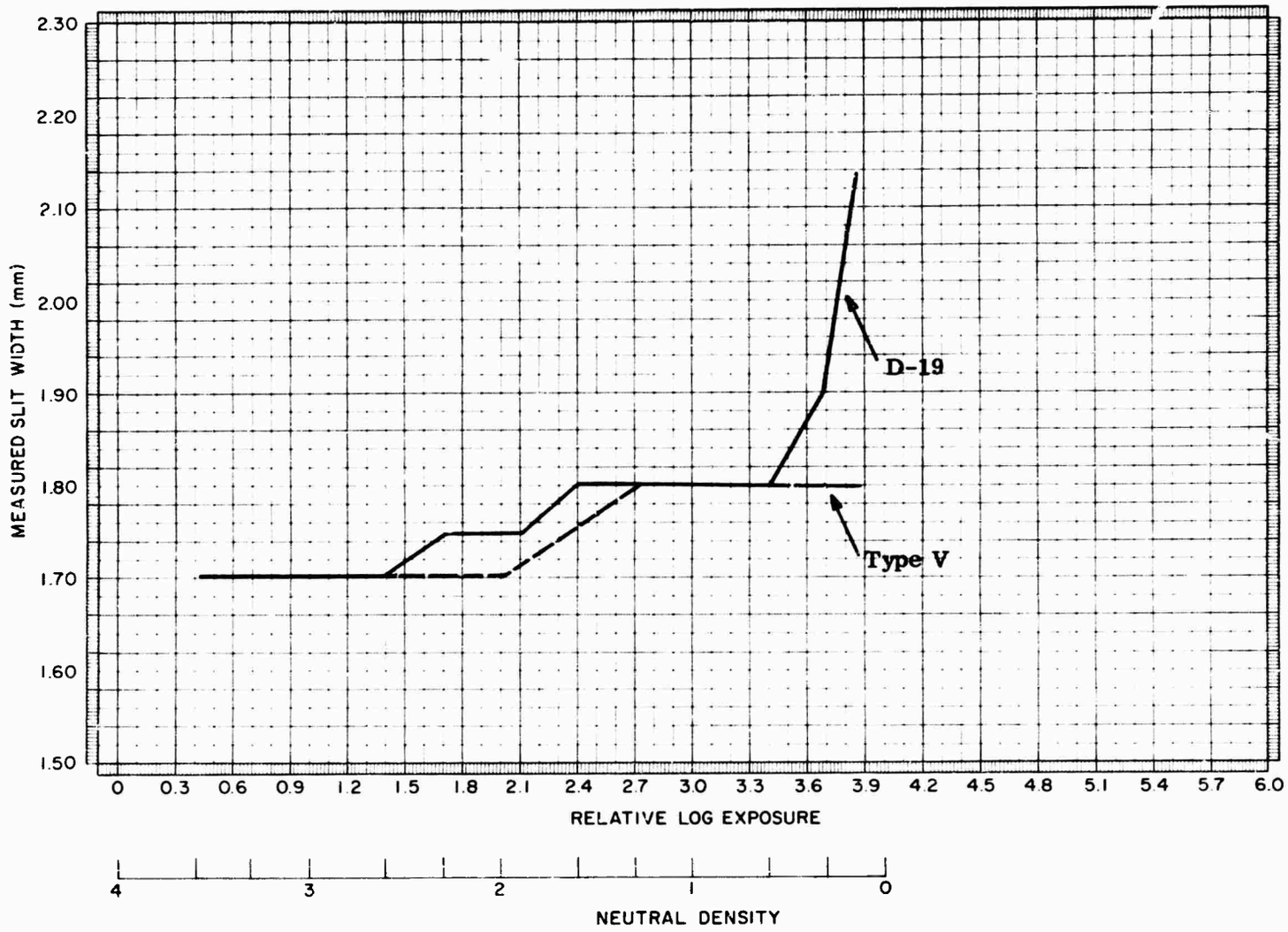

Infrared film as the example, since in many respects this film is of the most interest to the sponsor.

In Figure 24 we show a series of superimposed traces of slit exposures made with High Speed Infrared film through a 47 (blue) filter and developed in D-19. On the horizontal coordinate of Figure 24 we draw the original dimensions of the film plane (using the 50:1 ratio of the instrument). On the vertical coordinate, we plot specular density as determined from the calibration wedge of the microdensitometer. This density is only approximately equal to the usual diffuse density measured in a normal densitometer.

Using the fluctuations of the density trace as a measure of granularity, we see a sharp increase in the granularity of the developed film as the average density increases. For example, the increment of detectivity between the density lines for ND = 0 and ND = 0.6 is only one or two granularity, or $\sigma(D, A)$, increments. In fact, if the ND = 0.3 curve were included in Figure 24, it would overlap both the ND = 0 and ND = 0.6 curves to give a confusing picture. At lower densities, the fluctuations are smaller and the number of recordable increments increases.

Let us now look at the linear dimensions of the slit widths as revealed by the traces of Figure 24. We see that up to exposure values of ND = 1.0 (specular density of 2.0) the shoulders of the edges are not too extreme, and that a measurement based on the top of the shoulder is moderately accurate (1.70 mm). At the two highest densities of Figure 24 the shoulders are very broad (see the micrographs of Figure 17), and measurement of the slit width from the top of the shoulder will be in error. At low power (Figure 17), the shoulders appear to be too dense to make a meaningful measurement of the slit width.

Let us now consider the microdensitometer traces of High Speed Infrared film, exposed through a 47 filter and developed in Type IV, as shown in Figure 25. Observe that the horizontal dimension scale of Figure 25 is the same as that for Figure 24 (50:1 ratio) but that the density scale for the Type IV developer is expanded. The low granularity of these traces, compared to those of Figure 24, even at the same value of specular density, is quite apparent. It is clear that the ND = 0.3 curve could easily be placed on Figure 25 without overlapping with the ND = 0 or the ND = 0.6 curves, indicating a considerable increase in detectivity for the Type IV film compared to the D-19 film.

The traces of Figure 25 appear to make the dimensional reading of the slit width easy. However, that is not the case; the shoulders of all the curves of Figure 25 are quite broad, which in fact we take to be a sign of the increased detectivity of the film processed in Type IV. However, we note an edge or adjacency effect on all these traces that was apparent in the micrographs of Figure 17, and which made low-power reading of the slit dimensions quite accurate. On the microdensitometer traces of Figure 25, a good estimate of the slit width can be made from peak to peak of the edge traces.

To better compare the detectivity of films processed in Type IV and D-19, we show in Figure 26 a set of traces run at a smaller scanning aperture (5 μ) and with a constant density scale. We illustrate this effect with High Speed Infrared film exposed through an 89B filter at moderate exposures of ND = 2.0 and ND = 2.3. The D-19 scans of Figure 26 show a fluctuation of about 6mm = 0.13 density unit. The density increment between the two D-19 traces is only about 12 mm, or two density fluctuation

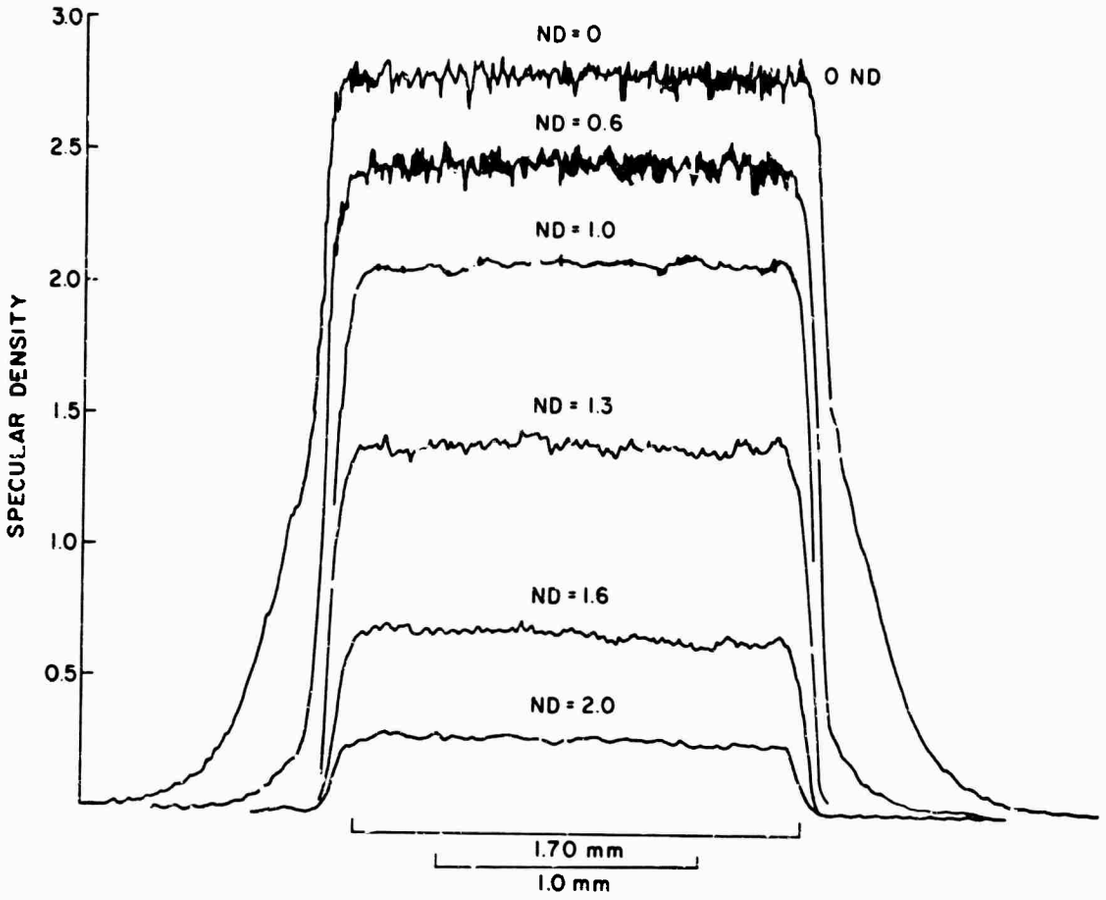

Figure 24. Microdensitometer Traces of Slit Exposures of High-Speed Infrared Film Made Through a 47 Filter and Developed in D-19

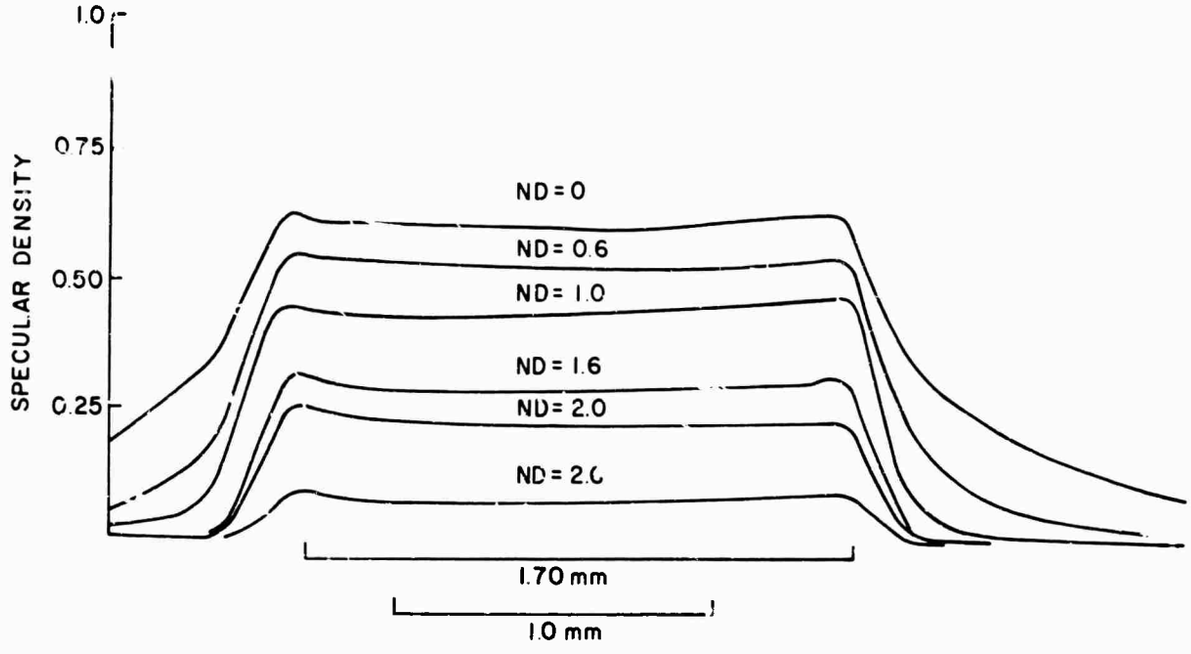

Figure 25. Microdensitometer Traces of Slit Exposures of High-Speed Infrared Film Made Through a 47 Filter and Developed in Type IV

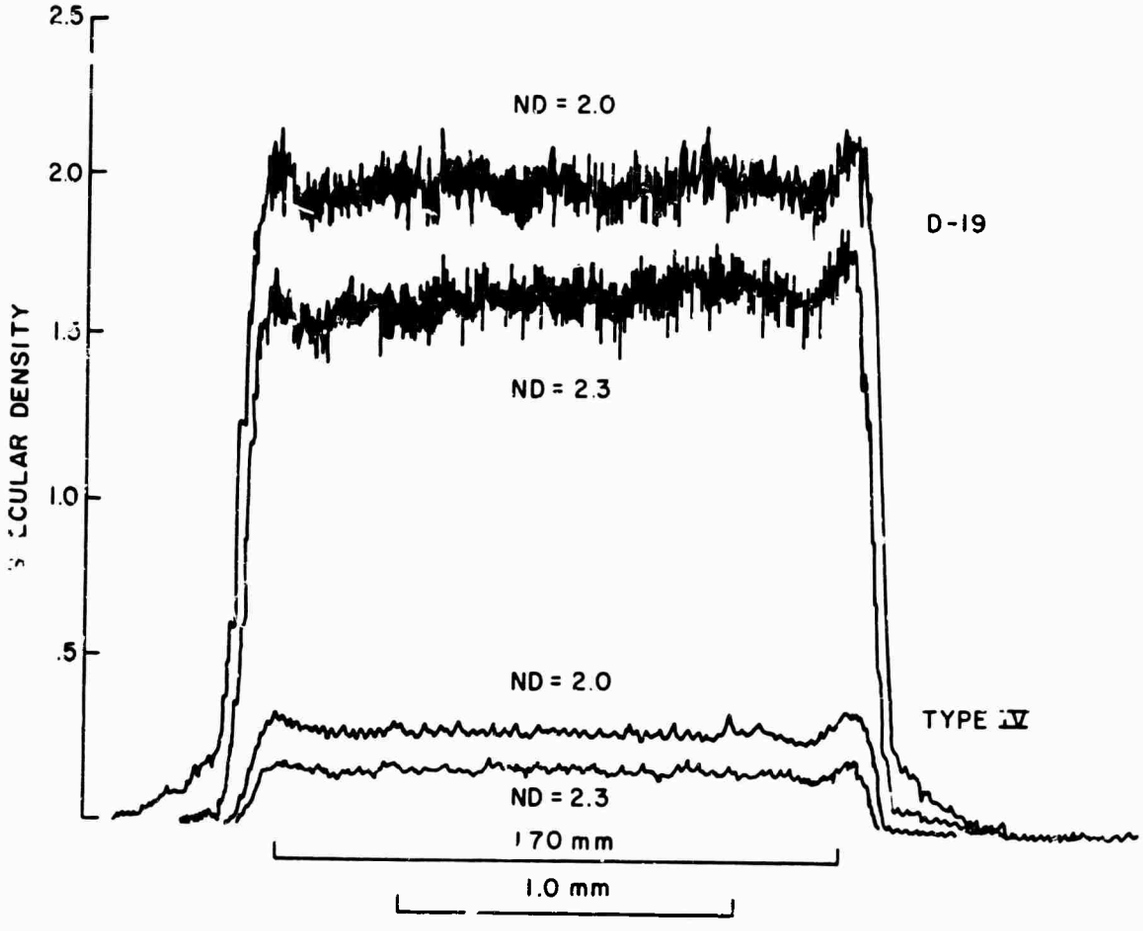

Figure 26. Comparison of Microdensitometer Traces of Slit Exposures of High-Speed Infrared Film Made Through an 89B Filter and Developed in D-19 and Type IV

units. Consider now the two Type IV traces. The density fluctuation is only about 1 mm or 0.02 density unit. The separation between the two traces is about 5 mm, or about 5 density fluctuation units. Let us use the formula of Eq. (14) to calculate the difference in detectivity, at this exposure level, for the films processed in these two developers. From Table I, we see that the D-19 and Type IV gammas for High Speed Infrared film are about 2.0 and 0.5, respectively. The ratio of $\sigma(D, A)$ for the two films is approximately the ratio of the fluctuations or 6 mm/1 mm. Therefore, the ratio of the detectivity of the Type IV film to the D-19 film is approximately:

$$d_4/d_{19} = (0.5/1) \times (2.0/6 = 1.5) ,$$

or a 50% improvement in detectivity.

We realize that the approximate estimations of granularity from the traces of Figure 26 are not accurate, and that an accurate determination of gamma for the two films would require a careful correlation between the specular densities of Figure 26 and the diffuse densities on which the characteristic curve is based. However, the approximate calculation of the ratio of detectivities indicates that the XDR developer can give improved detectivity over that of the normal active developer.

At present, Lincoln Laboratory is analyzing calibration exposures that have been processed in control and XDR developers. We hope that other laboratories will also check out the use of XDR developers in field application for the reduction of flare. We would hope that the results from such calibrations and field tests will substantiate our observation that XDR developers increase detectivity.

REFERENCES

1. RADC, AF30(602)-3227.

2. W. Kammerer, L. Corben, and others, "Extended Dynamic Range Process," Technical Operations, Inc., Report No. TO-B 67-37 (RADC-TR-67-431) (1967).

3. A. Shepp, S.P.S.E. News 10, 5 (1967).

4. H.J. Zweig, J. Opt. Soc. Am. 46, 805 (1956).

5. H. Frieser, Phot. Sci. Eng. 3, 164 (1959).

6. G.C. Higgins and K.F. Stulty, J. Opt. Soc. Am. 49, 925 (1959).

7. H.J. Zweig, G.C. Higgins, D.L. MacAdam, J. Opt. Soc. Am. 48, 926 (1958).

Unclassified

Security Classification

DOCUMENT CONTROL DATA - R&D

(Security classification of title, body of abstract and indexing annotation must be entered when the overall report is classified)

1. ORIGINATING ACTIVITY *(Corporate author)*
Technical Operations, Inc.
South Avenue
Burlington, Massachusetts 01803

2a. REPORT SECURITY CLASSIFICATION
Unclassified

2b. GROUP

3. REPORT TITLE

EXTENDED DYNAMIC RANGE PROCESSING

4. DESCRIPTIVE NOTES *(Type of report and inclusive dates)*
Scientific. Final. 10 October 1966 Approved 22 Nov. '67 10 October 1967

5. AUTHOR(S) *(Last name, first name, initial)*
A. Shepp
W. Kammerer
R. Shuman

6. REPORT DATE	7a. TOTAL NO. OF PAGES	7b. NO. OF REFS
November, 1967	55	7

8a. CONTRACT OR GRANT NO. ARPA Order No. 450 F1962867C0082	9a. ORIGINATOR'S REPORT NUMBER(S) TO-B 68-6
b. PROJECT AND TASK NO. Work Unit Nos. 8663-00-01	
c. DOD ELEMENT 6250301R	9b. OTHER REPORT NO(S) *(Any other numbers that may be assigned this report)* AFCRL-67-0633
d. DOD SUBELEMENT n/a	

10. AVAILABILITY/LIMITATION NOTICES
Distribution of this document is unlimited. It may be released to the Clearinghouse, Department of Commerce, for sale to the general public.

11. SUPPLEMENTARY NOTES	12. SPONSORING MILITARY ACTIVITY
This research was supported by the Advanced Research Projects Agency	Air Force Cambridge Research Laboratories (CRO), L.G. Hanscom Field Bedford, Massachusetts 01730

13. ABSTRACT

Four Kodak films — Pan-X, Plus-X, Tri-X, and High-Speed Infrared — were exposed to slit images (1.7 x 14 mm) over a range of 10^4 E. Samples were developed in D-19 and D-76 for high- and low-contrast control and in three Tech/Ops extended dynamic range (XDR) developers — E-20A, E-20B, and Type IV. Subsequent analyses showed that the XDR developers produce lower granularity than the control developers and thus greatly reduce the apparent flare and increase detectivity, even at low density and gamma.

DD FORM 1 JAN 64 1473

Unclassified

Security Classification

14. KEY WORDS	LINK A		LINK B		LINK C	
	ROLE	WT	ROLE	WT	ROLE	WT
Film Processing Film Flare Extended Dynamic Range Developers						

INSTRUCTIONS

1. ORIGINATING ACTIVITY: Enter the name and address of the contractor, subcontractor, grantee, Department of Defense activity or other organization *(corporate author)* issuing the report.

2a. REPORT SECURITY CLASSIFICATION: Enter the overall security classification of the report. Indicate whether "Restricted Data" is included. Marking is to be in accordance with appropriate security regulations.

2b. GROUP: Automatic downgrading is specified in DoD Directive 5200.10 and Armed Forces Industrial Manual. Enter the group number. Also, when applicable, show that optional markings have been used for Group 3 and Group 4 as authorized.

3. REPORT TITLE: Enter the complete report title in all capital letters. Titles in all cases should be unclassified. If a meaningful title cannot be selected without classification, show title classification in all capitals in parenthesis immediately following the title.

4. DESCRIPTIVE NOTES: If appropriate, enter the type of report, e.g., interim, progress, summary, annual, or final. Give the inclusive dates when a specific reporting period is covered.

5. AUTHOR(S): Enter the name(s) of author(s) as shown on or in the report. Enter last name, first name, middle initial. If military, show rank and branch of service. The name of the principal author is an absolute minimum requirement.

6. REPORT DATE: Enter the date of the report as day, month, year, or month, year. If more than one date appears on the report, use date of publication.

7a. TOTAL NUMBER OF PAGES: The total page count should follow normal pagination procedures, i.e., enter the number of pages containing information.

7b. NUMBER OF REFERENCES: Enter the total number of references cited in the report.

8a. CONTRACT OR GRANT NUMBER: If appropriate, enter the applicable number of the contract or grant under which the report was written.

8b, 8c, & 8d. PROJECT NUMBER: Enter the appropriate military department identification, such as project number, subproject number, system numbers, task number, etc.

9a. ORIGINATOR'S REPORT NUMBER(S): Enter the official report number by which the document will be identified and controlled by the originating activity. This number must be unique to this report.

9b. OTHER REPORT NUMBER(S): If the report has been assigned any other report numbers *(either by the originator or by the sponsor)*, also enter this number(s).

10. AVAILABILITY/LIMITATION NOTICES: Enter any limitations on further dissemination of the report, other than those imposed by security classification, using standard statements such as:

(1) "Qualified requesters may obtain copies of this report from DDC."

(2) "Foreign announcement and dissemination of this report by DDC is not authorized."

(3) "U. S. Government agencies may obtain copies of this report directly from DDC. Other qualified DDC users shall request through

_____."

(4) "U. S. military agencies may obtain copies of this report directly from DDC. Other qualified users shall request through

_____."

(5) "All distribution of this report is controlled. Qualified DDC users shall request through

_____."

If the report has been furnished to the Office of Technical Services, Department of Commerce, for sale to the public, indicate this fact and enter the price, if known.

11. SUPPLEMENTARY NOTES: Use for additional explanatory notes.

12. SPONSORING MILITARY ACTIVITY: Enter the name of the departmental project office or laboratory sponsoring *(paying for)* the research and development. Include address.

13. ABSTRACT: Enter an abstract giving a brief and factual summary of the document indicative of the report, even though it may also appear elsewhere in the body of the technical report. If additional space is required, a continuation sheet shall be attached.

It is highly desirable that the abstract of classified reports be unclassified. Each paragraph of the abstract shall end with an indication of the military security classification of the information in the paragraph, represented as *(TS), (S), (C), or (U).*

There is no limitation on the length of the abstract. However, the suggested length is from 150 to 225 words.

14. KEY WORDS: Key words are technically meaningful terms or short phrases that characterize a report and may be used as index entries for cataloging the report. Key words must be selected so that no security classification is required. Identifiers, such as equipment model designation, trade name, military project code name, geographic location, may be used as key words but will be followed by an indication of technical context. The assignment of links, rules, and weights is optional.

TECHNICAL OPERATIONS, INCORPORATED

NORTHWEST INDUSTRIAL PARK
BURLINGTON, MASSACHUSETTS 01803
(617) 272-2000

26 February 1968

Gentlemen:

Table No. 1, report AFCRL-67-0633, p. 4 has been revised to incorporate changes in quantity of chemicals and the recommended chemicals to be used in preparation in the Extended Range Developers.

Sincerely,

William J. Kammerer

William J. Kammerer
Project Leader

TABLE 1

DEVELOPER FORMULATIONS USED IN THIS REPORT

(g/litre)

Formulation (In Order of Solution)	T/O XDR Developers ***			Kodak Developers	
	E-20A	E-20B	Type IV	D-19	D-76
Water	800 cc	800 cc	800 cc	-	-
K_2SO_3*	25	50	25	-	-
Kodak Na_2SO_3	-	-	-	90.0	100.0
Metol (Elon)†	0.5 ± 0.1	0.5 ± 0.1	1.0 ± .2	2.0	2.0
Hydroquinone (HQ)**	0.5 ± 0.1	0.5 ± 0.1	1.0 ± .2	8.0	5.0
$KHCO_3$‡	-	-	10.0 ± .5	-	-
Kodak Na_2CO_3, (sodium carbonate)	-	-	-	52.5	-
Kodak Borax, granular	-	-	-	-	2.0
Kodak KBr (potassium bromide)	-	-	-	5.0	-
Water to 1 liter					
Kodak Film Type	Recommended T/O Developer			Kodak Emulsion No. Test Films	
Pan-X	X		X	5060-36-1	
Plus-X			X	5061-530-16	
Tri-X			X	5063-479-34	
High Speed IR		X		5218-101-4	

*Potassium Sulfite - Matheson Coleman and Bell, purified grade

†Metol (Elon) - Graphol, Philip J. Hunt, Inc.

**Hydroquinone - Fisher Chemical Corporation, purified grade

‡Potassium bicarbonate - Fisher Chemical Corporation, purified grade

***E-20A; E-20B-pH 9.0; Type IV-pH 8.6